Working paper

2023-08

Statistics and Econometrics
ISSN 2387-0303

Modelling intervals of minimum/maximum temperatures in the Iberian Peninsula

Gloria González-Rivera, Vladimir Rodríguez-Caballero, Esther Ruiz

uc3m | Universidad Carlos III de Madrid

Modelling intervals of minimum/maximum temperatures in the Iberian Peninsula*

Gloria González-Rivera
Department of Economics, University of California, Riverside

Vladimir Rodríguez-Caballero
Department of Statistics, ITAM (Mexico)
and CREATES, Aarhus University (Denmark)

Esther Ruiz†
Department of Statistics, Universidad Carlos III de Madrid

10th July 2023

Abstract

In this paper, we propose to model intervals of minimum/maximum temperatures observed at a given location by fitting unobserved component models to bivariate systems of center and log-range temperatures. In doing so, the center and log-range temperature are decomposed into potentially stochastic trends, seasonal and transitory components. We contribute to the debate on whether the trend and seasonal components are better represented by stochastic or deterministic components. The methodology is implemented to intervals of minimum/maximum temperatures observed monthly in four locations in the Iberian Peninsula, namely, Barcelona, Coruña, Madrid and Seville. We show that, at each location, the center temperature can be represented by a smooth integrated random walk with time-varying slope while the log-range seems to be better represented by a stochastic level. We also show that center and log-range temperature are unrelated. The methodology is then extended to model simultaneously minimum/maximum temperatures observed at several locations. We fit a multi-level dynamic factor model to extract potential commonalities among center (log-range) temperature while also allowing for heterogeneity in different areas. The model is fitted to intervals of minimum/maximum temperatures observed at a large number of locations in the Iberian Peninsula.

*Financial Support from "la Caixa" Foundation, grant LCF/PR/SR20/52550012-Climate change and economic challenges for the Spanish society, is gratefully acknowledged. The third author also acknowledges financial support from the Spanish Government grant PID2019-108079GBC21/AIE/10.13039/501100011033 (MINECO/FEDER). The support of Jouni Helske with some of the codes used in this paper is also gratefully acknowledged. We are also grateful to participants at the 69th International Symposium of Forecasters (July, 2022), Rome-Waseda Time Series Symposium (October, 2022) and 16th International Conference, Computational and Financial Econometrics (December, 2022). Any remaining errors are obviously our responsibility.

†Corresponding author. E-mail: ortega@est-econ.uc3m.es

Keywords: Climate change, Dynamic Factor Models, Interval valued time series, State space models

JEL codes: C22, C32, C53, Q54.

> What we find more difficult to talk about is our deep dissatisfaction with the ability of our models to inform society about the pace of warming, how this warming plays out regionally, and what it implies for the likelihood of surprises.
>
> *Palmer and Stevens (2019)*

1 Introduction

Climate change can be defined as the variation in the joint probability distribution that describes the state of the atmosphere, oceans, and fresh water including ice; see Hsiang and Kopp (2018). According to the latest fifth and sixth assessment reports of the International Panel for Climate Change (IPCC, 2014, 2022), one of the most important aspects of climate change is global warming, described by the evolving distribution of temperature.

The stand of the literature using econometric models to describe the evolution of temperature focuses on average temperature, which is obviously an important characteristic of the distribution.[1] However, average temperature alone is not enough to reflect the complicated variations of climate. In an early paper, Katz and Brown (1992) show that the frequency of extreme weather events is relatively more dependent on any changes in the variability than on the mean of temperature, with this sensitivity being relatively greater the more extreme the event. Consequently, policy makers should not rely on scenarios of future temperature involving only changes in means.

Our paper contributes to the important literature on time series modelling of temperatures in two main ways. First, instead of analysing average temperatures, we use the rich joint information contained in the interval of minimum/maximum temperature, analysing them as IVTS. By doing so, we add to the information of the average tempera-

[1] Although, we focus on econometric models, there is a large literature based on deterministic climate models; see Diebold and Rudenbush (2022b) for a comparison between both types of models in the context of measuring ice volume in the Arctic.

ture, represented by the center of the interval, the information about the range between the maximum and minimum temperatures and, consequently, information associated to extreme temperatures.

In particular, we propose using a state space representation of the non-stationary and seasonal center and log-range temperature in which both the trend and seasonal components can be stochastic; see Harvey (1997) about the advantages of using unobserved components models instead of widely used VAR models based on differencing and cointegration and Pretis and Hendry (2013), who suggest using a state-space approach due to the conflicting results often encountered when unit root and cointegration tests are used in the context of monthly data. The unobserved component models framework allows us to decide about the nature of the trends and seasonal components of the center and log-range temperatures, using the Kalman filter and smoothing (KFS) algorithms to extract the components together with their uncertainty. Structural time series models have been proposed before in the context of average temperatures by, for example, Bloomfield (1992), Woodward and Gray (1993) and Zheng and Bahsher (1999) for annual data and by Good *et al.* (2007) and Proietti and Hillebrand (2017) for monthly data and Stern and Kaufmann (2000) for annual temperatures in the Northern and Southern Hemispheres. Our methodology is closely related with the smoothing procedure proposed by Maia and Carvalho (2011), who fit two independent models to the mid-points and ranges of the intervals and estimate the smoothing parameters by minimizing the interval sum of one-step-ahead forecast errors; see Harvey and Jaeger (1993), who show that the steady-state Kalman filter for the local linear trend model takes the form of Holt's recursions with suitably defined smoothing constants. However, these latter authors do not consider the seasonal component.

Finally, to deal with the heterogeneity in the joint evolution of minimum/maximum temperatures observed at various locations, we propose using a multi-level Dynamic Factor Model (ML-DFM), which is estimated using the KFS algorithms. The ML-DFM allows to represent the joint evolution of a large system of time series of center/log-range temperatures assuming that some of the trends are common to all locations while others may be common to some subsets of locations. Consequently, ML-DFM can represent some commonality in the evolution of temperatures while allowing, at the same time, for

some idiosyncratic movements that explain the heterogeneity often observed.

Our second contribution is the empirical analysis of monthly IVTS of minimum/maximum temperatures observed at 68 locations spread all over the Iberian Peninsula over nearly a century from January 1930 to December 2020. This analysis is of particular interest because of the severe heat waves experienced in Southern Europe in recent years; see, for example, Kew *et al.* (2017). After analysing minimum/maximum temperatures separately in four selected locations, namely Barcelona, Coruña, Madrid and Seville, we show that the main characteristics of the center temperature in each of these four cities can be represented by a smooth stochastic trend. The fact that the slope of the trend changes over time can explain why some authors find upward trends while others conclude about the hiatus in warming (global mean temperature has not risen significantly over the last two decades). Furthermore, we observe some heterogeneity in the trends of these four cities, with the slope of the trend at the end of the observation period, in December 2020, being different in the four cities considered. In particular, the slope of the trend is larger in Barcelona and smaller in Seville. We also show that the seasonal component of the center temperatures has a stochastic behaviour. When looking at the log-range, we conclude that it can be represented by a stochastically evolving level with stochastic seasonality. As expected, at the end of the sample period, the log-range is clearly larger in the two cities in the interior of the Iberian Peninsula, Madrid and Seville, and smaller in the two coastal cities, Barcelona and Coruña. Another important conclusion from the empirical analysis of the center and log-range temperatures in these four cities is that, in each of them, the center and log-range temperatures are not correlated, allowing to model both characteristics separately.

The rest of this paper is organized as follows. In Section 2, we briefly survey the literature using econometric models to describe the dynamic evolution of temperatures and the still open debates in this literature. Section 3 describes the methodology proposed to model IVTS of minimum/maximum temperature. In particular, we describe how to model and forecast temperature intervals at a given location using state space models and the Kalman filter to estimate trends and seasonal components. We also describe ML-DFM and the implementation of KFS to extract the common factors. Section 4 describes the data and the main empirical characteristics of the IVTS of the center/log-range systems

at Barcelona, Coruña, Madrid and Seville. Section 5 fits state-space models to extract trends and seasonal components in each of these four locations of the Iberian Peninsula. Finally, Section 6 concludes the paper with a summary of the main conclusions.

2 Open debates on the econometric modelling of temperatures

When describing global warming, the interest is on the distribution of temperature either a given location or jointly at several locations. However, the stand literature focus on analysing the evolution of average temperature, i.e. the central tendency of the distribution, with a large variety of statistical and econometric approaches, periods and frequency of observation, and locations to analyse it. Many of these studies find an upward trend in average temperatures. Increasing trends are found by, for example, Deng and Fu (2019), who compare several methods for extracting cycles from daily temperatures, and Barbosa, Scotto and Alonso (2011), who also analyse daily temperatures in several locations at Central Europe. These latter authors use quantile regressions to fit linear trends to the quantiles of average daily temperature at each location. Note that, by doing this, they are analysing the distribution of average temperature but not the distribution of temperature it self. Similarly, Scotto, Barbosa and Alonso (2011) use Extreme Value Theory (EVT) to analyse the extremes of the distribution of daily average temperature in Europe and the spatial distribution of extreme events; see also Wang *et al.* (2021), who use Generalized EVT to look for fingerprints on temperatures. A similar approach is considered by Gadea Rivas and Gonzalo (2020, 2022), who use regressions to estimate the full cross-sectional distribution of average temperatures or the distribution of average daily temperatures within a given year. A very similar approach is taken by Chang *et al.* (2020), who construct densities of global average temperatures in the Southern Hemisphere (measured as anomalies with respect to average temperatures over the base period 1961-90) and conclude that there is more persistence in the mean while non-stationarity is less evident in the variance. Although most evidence is about average temperature having an upward increasing trend, it is important to point out that several authors describe what is known as the hiatus in warming; see, for example, Schmidt, Shindell and

Tsigaridis (2014), Pretis, Mann and Kaufmann (2015), Medhaug *et al.* (2017) and Miller and Nam (2020).

Although the literature focusing on average temperature is obviously relevant, there is some agreement about average temperature alone not being enough to reflect the complicated variations of climate. In an early paper, Katz and Brown (1992) show that the frequency of extreme wheather events is relatively more dependent on any changes in the variability than on the mean of climate, with this sensitivity being relatively greater the more extreme the event. Consequently, policy makers should not rely on scenarios of future climate involving only changes in means. In this direction, on top of modelling average temperature, several authors have considered modelling the evolution of range temperature, computed as the difference between the maximum and minimum temperatures within a given period of time. These studies often find a downward trend in temperature variability although the evidence is not as clear as for the positive trend of average temperature. For example, Vose, Easterling and Gleason (2005), Dupuis (2014), Qu, Wan and Hao (2014) and Meng and Taylor (2022) show that increases in minimum temperatures have been more important than increases in maximum temperatures in the globe (the first), different regions of the US (the second and third), and four cities in Spain (the last). Xu *et al.* (2013) analyse minimum and maximum daily temperatures in 825 stations in China observed from 1951 to 2020, and conclude that the diurnal temperature range has significantly decrease at 49% of the stations, with significant increases being identified at 3% of them. Diebold and Rudebusch (2022a) propose modelling both the average and range temperature using separate regressions with deterministic trends, seasonal dummies and their interactions. The two univariate models are fitted to average and range temperatures observed daily in selected cities in the US since 1960 to 2017. Instead of considering separate regressions, Meng and Taylor (2022) propose two alternative methods to model IVTS of minimum and maximum temperature. First, they propose modelling each of the two time series separately by fitting models with deterministic trends and seasonal components and allowing for interactions between minimum and maximum temperatures. Alternatively, IVTS of minimum and maximum temperature are modelled by a bivariate VARMA-MGARCH model. Using daily data in four Spanish cities observed from 1951 to 2015, their results also suggest a decrease in the diurnal

temperature range and an increase in trend. Note that they do not restrict the model to avoid crossing of minimum and maximum temperature at a given moment of time. The authors recognise that, although unlikely, the temperatures may cross.

Several important debates about modelling the dynamic characteristics of average and range temperature are going on in the related literature. First, there is a growing literature about the nature of the trend in temperature; see, for example, the discussion by Proietti and Hillebrand (2017). Within this literature, one of the most important controversies is about whether trends in temperatures (or other climatological variables) should be modelled by assuming that they are deterministic, as it is often done by many authors, or stochastic. For example, Fatichi *et al.* (2009) examine trends of daily average temperatures recorded in 26 stations in Tuscany (Italy) and conclude that only for a subset of 9 stations a deterministic trend can be regarded as the most appropriate model. Kaufmann, Kauppi and Stock (2010), Kaufmann *et al.* (2013) and Chang *et al.* (2020) are also among those who support the presence of stochastic trends in temperatures. However, Gao and Hawthorne (2006), Gay, Estrada and Sánchez (2009) and Gadea Rivas and Gonzalo (2020, 2022) argue that temperature series are better characterized by trend-stationary processes. Furthermore, more recently, Chen, Gao and Vahid (in press) support that global temperature can be represented by deterministic non-linear trends. Seidel and Lanzante (2004), Estrada, Gay and Sánchez (2010), Pretis and Allen (2013), Estrada, Perron and Martínez-López (2013), Friedrich *et al.* (2020) and Kim *et al.* (2020) further propose models with deterministic trends with breaks, while Friedrich, Smeekes and Urbain (2020) and Friedrich *et al.* (2020) propose smooth non-parametric trends.[2] There are also several proposals of modelling temperatures based on long-memory models; see, for example, Baillie and Chung (2002), Gil-Alana (2005), Ventosa-Santaularia, Heres and Martínez-Hernández (2014), Mangat and Reschenhofer (2020) and Vera-Valdés (2021).

On top of trends, seasonal variation is the most prominent source of climate variability, so climate change could also be reflected in it; see Pezzulli, Stephenson and Hannachi

[2]It is important to note that it is extremely difficult to stablish the nature of trend in a time series with a finite sample and, consequently, there is still a debate about the power of tests for trend-stationarity or difference-stationarity; see, for example, the general discussions by Diebold and Senhadji (1996), Phillips (2005, 2010) and Rao (2010) and the comments by Stern and Kaufmann (2000) and Pretis and Hendry (2013) in the particular context of climate variables.

(2005) and Proietti and Hillebrand (2017) for its importance. Consequently, there is also an interest about knowing the most appropriate model for the seasonal components of temperature.

Finally, among the hazards encountered when modelling climate-related time series, Pretis and Hendry (2013) point out the spatial variation of temperature trends, suggesting that there may be unmodelled heterogeneity when this variability is not taken into account. Dupuis (2014) and Scotto, Barbosa and Alonso (2011) also find heterogeneity, analysing minimum and maximum temperatures observed in 12 locations in Southwestern US and extremes in average daily temperature in Europe, respectively. Recently, Estrada, Kim and Perron (2021) contribute to this debate by showing that the response of high-latitudes to increases in radiative forcing is much larger than elsewhere in the world, with a warming more than twice the global average. Other authors finding different trends in average temperature depending on the location are Chang *et al.* (2020), Holt and Teräsvirta (2020) and Gadea Rivas and Gonzalo (2022).[3] The heterogeneity in climate change may have important consequences for policy makers; see Kaufmann *et al.* (2017), who argue that the scepticism about climate change could partially being caused by the spatial heterogeneity of climate change, and Zaval *et al.* (2014) and Binelli, Loveless and Schaffuer (in press), who causally link perceived changes in local temperature to changes in global warming beliefs. Holt and Teräsvirta (2020) generalize univariate smooth transition models providing a multivariate generalization of the shifting-mean autoregressive model to test and model whether series co-shift. They find evidence of co-shifting of hemispheric temperatures which aligns with earlier evidence of Kaufmann and Stern (1997) on the co-movement of hemispheric temperature evolution and the anthropogenic character of climate change.

When modelling minimum/maximum temperature at several locations, one would need to deal with non-stationary and potentially cointegrated VARs with strong seasonal patterns; see, for example, Cheung (2007), Cheung, Cheung and Wan (2009) and Caporin, Ranaldo and Santucci de Magistris (2013), who suggest cointegrated VAR models for

[3]It is also important to remark that, although in this paper we focus on urban stations, it could also be interesting to extend the analysis to non-urban ones; see, for example, Hausfather *et al.* (2013) for an analysis of the impact of urbanization on temperature trends and the discussion by Estrada and Perron (2021).

IVTS in the context of non-seasonal high and low financial prices.[4] However, estimation of seasonally cointegrated VAR models could be rather difficult; see, Darné (2004) for a seasonal cointegrated model for monthly data and Seong *et al.* (2008) for issues related with misspecification of cointegrating ranks. Cubadda (1999) for the alternative and more complicated representation of seasonal cointegrated multivariate time series and He *et al.* (2019, 2021) for seasonal VAR models with shifting means and covariances for monthly temperatures.

3 State space models to represent temperature IVTS

In this section, we describe the methodology proposed to represent temperature IVTS, which is based on unobserved components time series models and the use of the Kalman filter and smoothing (KFS) algorithms to extract the unobserved trends and seasonal components of the center/log-range temperatures. We first describe the models used to represent center/log-range temperatures at a given location and, second, the ML-DFM designed to represent them at several locations simultaneously.

3.1 Univariate models: temperature intervals at a given location

It is important to take into account that IVTS models used to represent and predict the temporal evolution of minimum/maximum temperature should be restricted in such a way that the predicted maxima and minima do not cross. Consequently, in order to avoid the potential crossing of minimum and maximum temperatures, we follow González-Rivera, Luo and Ruiz (2020) and model the system of center/log-range at a particular location. Denote by $X_t = (C_t, R_t)'$, the 2×1 vector of the center and log-range temperature observed

[4] Alternatively, Maia and de Carvalho (2011) propose using multilayer perceptone neural networks and exponential smoothing for non-stationary IVTS, while Xiong, Bao and Hu (2014) and Xiong, Li and Bao (2017) use support vector regression and compare forecasts obtained using several procedures, among them smoothing and cointegrated VARs. Although the procedure proposed by these latter authors have good performance in terms of the interval average relative variance, the computational effort is rather heavy. Recently, Zhang *et al.* (2020) have also proposed a hybrid model combining cointegrated VAR models with AI to model intervals of pork prices. Alternatively, He *et al.* (2021) propose modelling non-stationary IVTS using Autoregressive Conditional Internal (ACI) models. However, these models are not taking into account the strong seasonality observed in temperature data.

at a particular location at time t, which is modelled as the sum of the vector of trends, $\mu_t = (\mu_{1t}, \mu_{2t})'$, the vector of seasonal components, $\gamma_t = (\gamma_{1t}, \gamma_{2t})'$, and the vector of irregular components, $\varepsilon_t = (\varepsilon_{1t}, \varepsilon_{2t})'$. Consider the following bivariate Frequency-Specific Basic Structural Model (FS-BSM), with stochastic trends and seasonal components

$$X_t = \mu_t + \gamma_t + \varepsilon_t, \tag{1a}$$

$$\mu_t = \mu_{t-1} + \beta_{t-1} + \eta_t, \tag{1b}$$

$$\beta_t = \beta_{t-1} + \zeta_t, \tag{1c}$$

$$\gamma_t = \sum_{j=1}^{6} \gamma_t^{(j)}, \tag{1d}$$

$$\gamma_t^{(j)} = \gamma_{t-1}^{(j)} cos\lambda_j + \gamma_{t-1}^{*(j)} sin\lambda_j + \omega_t^{(j)}, \tag{1e}$$

$$\gamma_t^{*(j)} = -\gamma_{t-1}^{(j)} sin\lambda_j + \gamma_{t-1}^{*(j)} cos\lambda_j + \omega_t^{*(j)}, \tag{1f}$$

where $\lambda_j = \frac{\pi j}{6}$, $j = 1, ..., 6$, are the seasonal frequencies in radians and $\beta_t = (\beta_{1t}, \beta_{2t})'$ is the vector of time varying slopes of the trends. ε_t is assumed to be white noise with covariance matrix Σ_ε with the elements in the main diagonal, denoted by $\sigma_{1\varepsilon}^2$ and $\sigma_{2\varepsilon}^2$, representing the variances of the transitory component of the center and log-range, respectively. The off-diagonal element of Σ_ε, denoted by $\sigma_{12\varepsilon}$, represents the covariance between the transitory components of the center and log-range temperature. The vectors of noises of the levels, $\eta_t = (\eta_{1t}, \eta_{2t})$, of the slopes, $\zeta_t = (\zeta_{1t}, \zeta_{2t})'$, and of the seasonal components, $\omega_t^{(j)} = \left(\omega_{1t}^{(j)}, \omega_{2t}^{(j)}\right)$ and $\omega_t^{*(j)} = \left(\omega_{1t}^{*(j)}, \omega_{2t}^{*(j)}\right)$, are also assumed to be white noises with covariance matrices Σ_η, Σ_ζ, $\Sigma_\omega^{(j)}$ and $\Sigma_{\omega^*}^{(j)}$, respectively. The notation for the elements of these matrices and their interpretations are analogous to those used for the elements of Σ_ϵ. Note that γ_t^* appears as a matter of construction and its interpretation is not particularly important; see Harvey (1989) for a more detailed description. It is assumed that $\Sigma_\omega^{(i)} = \Sigma_{\omega^*}^{(i)}$ and that all disturbances in the model, ε_t, η_t, ζ_t, $\omega_t^{(j)}$, and $\omega_t^{*(j)}$ are mutually and serially uncorrelated at all lags and leads. Note that the covariances in the matrices $\Sigma_\varepsilon, \Sigma_\eta$, Σ_ψ and $\Sigma_\omega^{(i)}$ being all equal to zero, implies that the center and log-range temperatures can be modelled separately by fitting univariate FS-BSM models to each of them.

The univariate analogue of the FS-SBM in (1), which implies a seasonal component with six different variances, is described in detail by Hindrayanto *et al.* (2013). The BSM

popularized by Harvey (1989) is obtained when the variances of the seasonal shocks are equal to each other, i.e. $\sigma_{\omega}^{2(j)} = \sigma_{\omega}^2$, for $j = 1, ..., 6$. Finally, note that given the need of parsimony, and in the context of a univariate FS-BSM, Hindrayanto *et al.* (2013) propose to reduce the number of seasonal variances to two, which are denoted by σ_I^2 and σ_{II}^2. In our context, we reduce the number of seasonal covariance matrices to $\Sigma_{\omega}^{(I)} = \Sigma_{\omega}^{(1)}$ and $\Sigma_{\omega}^{(II)} = \Sigma_{\omega}^{(2)} = ... = \Sigma_{\omega}^{(6)}$. The trigonometric specification of the seasonal component is rather popular when modelling climate-related monthly data; see Campbell and Diebold (2005) and Dupuis (2012, 2014) for applications modelling the seasonal pattern of temperatures and Friedrich, Smeekes and Urbain (2020) and Friedrich *et al.* (2020) for seasonal patterns of ethane emissions.

Model (1) allows both the trend and seasonal components of the center and log-range to evolve stochastically. Furthermore, if $\sigma_{\zeta_1}^2 = 0$ ($\sigma_{\zeta_2}^2 = 0$), then the slope of the trend for the center (log-range) is constant and, therefore, $\beta_1 = ... = \beta_T = \beta$. If further, $\sigma_{\eta_1}^2 = 0$ ($\sigma_{\eta_2}^2 = 0$), then the trend is deterministic. Similarly, if the variances of the seasonal components, $\sigma_{\omega 1}^{2(I)}$, $\sigma_{\omega 2}^{2(I)}$, $\sigma_{\omega 1}^{2(II)}$ and $\sigma_{\omega 2}^{2(II)}$ are zero, then the seasonal components of the center and log-range temperatures are, respectively, deterministic.

If the parameters of the FS-SBM model in (1) were known, the Kalman filter and smoothing (KFS) algorithms can be implemented to extract one-step-ahead, filtered and smoothed estimates of the levels and seasonal components of the center and log-range.[5] However, the variances and covariances involved in model (1) are unknown and should be estimated before the KFS algorithms can be implemented. The parameters can be estimated by Maximum Likelihood (ML) based on the Kalman filter; see Harvey (1989) for a detailed description.

As discussed above, one important debate when modelling temperatures is whether trends are deterministic or stochastic. In the context of model ()1, testing for a deterministic trend can be carried out as proposed by Nyblom and Harvey (2000a). Different tests can be implemented depending on the particular model assumed for the trend. First, assuming that there is not seasonal component and the irregular component is white noise,

[5]Note that an appropriately modified Kalman filter can also be implemented to IVTS as proposed by Chen, Wang and Shieh (1997) and Ahn, Kim and Chen (2012). However, after transforming the interval into center and log-range, we implement the standard Kalman filter; see the Supplementary Appendix for details.

if $\sigma_\zeta^2 = 0$, i.e. the slope is constant, $\beta_t = \beta, \forall t$, they propose testing for a deterministic trend, i.e. $H_0 : \sigma_\eta^2 = 0$, using the following statistic

$$RW = \frac{1}{T\hat{\sigma_e^2}} \sum_{t=1}^{T} \left[\sum_{r=1}^{t} e_r \right]^2 , \tag{2}$$

where e_t are the Ordinary Least Squares (OLS) residuals of a regression of X_t on a constant and a deterministic time trend and $\hat{\sigma}_e^2 = \frac{1}{T} \sum_{t=1}^{T} e_t^2$. Under the null, if $\beta = 0$, RW has a Cramer von Mises (CvM) distribution with one degree of freedom, while, if $\beta \neq 0$, then it has a second-level CvM distribution. In this latter case, the statistic in (2) is denoted as RWD. Furthermore, in the context of the Integrated Random Walk (IRW), i.e. when $\sigma_\eta^2 = 0$, testing for a deterministic trend implies testing for $H_0 : \sigma_\zeta^2 = 0$. In this case, Nyblom and Harvey (2000a) propose the following statistic

$$IRW = \frac{1}{T^4\hat{\sigma}_e^2} \sum_{t=1}^{T} \left[\sum_{s=1}^{t} \sum_{r=1}^{2} e_r \right]^2 . \tag{3}$$

The critical values of the RW and IRW tests are reported by Harvey (2001). Note that, in the case of the IRW test, convergence to the asymptotic critical values is relatively slow and, consequently, using the asymptotic critical values can lead to the IRW test being oversized.

If the transitory component, ε_t, is not white noise, then one can use the same tests described above with e_t and $\hat{\sigma}_e^2$ substituted by ν_t and $\hat{\sigma}_\nu^2$, respectively, where ν_t are the standardized one-step-ahead errors and $\hat{\sigma}_\nu^2$ is their sample variance; see Harvey (2001) for a discussion.

Note that Nyblom and Harvey (2000a) point out that the tests above can be implemented in models that contain a non-stationary seasonal component.

Finally, when testing for a deterministic seasonal component can be carried out using the CvM seasonality test proposed by Harvey (2001) and Busetti and Harvey (2003). The CvM test statistic can be constructed using the one-step-ahead prediction errors from the model with parameters that are estimated under the null hypothesis. For $H_0 : \sigma_\omega^{2(j)} = 0$, the statistic follows a CvM distribution with two degrees of freedom for $j = 1, ..., 5$ and with one degree of freedom for $j = 6$; see Harvey (2001) for the critical

values. Furthermore, Hindrayanto *et al.* (2013) show that, in the model with two seasonal variances, the test for $H_0 : \sigma_\omega^{2(II)} = 0$ leads to a CvM test with nine degrees of freedom.

3.2 Multi-level Dynamic Factor Models

Consider now that the center/log-range temperature have been observed at each moment of time t at N locations. If the center and log-range temperatures at each location were mutually uncorrelated, then one could model separatelly the system of centers and the system of log-ranges. Consider, for example, the system of centers.[6] Given that our main interest is separating the common and heterogenous behaviour of the trends in the center temperatures at different locations, we consider the deseasonalized centers.[7] Denote by $Y_t = (y_{1t}, ..., y_{Nt})'$ the $N \times 1$ vector of deseasonalized centers. We follow Rodríguez-Caballero and Caporin (2019) and propose an innovative multi-level DFM what allows decomposing the factor structure into different levels, with some factors associated with the full cross-section of variables (pervasive factors), some other factors impacting a speci

c subset of variables (non-pervasive factors), and other factors impacting several subsets of variables (semipervasive factors). As proposed by Hallin and Liska (2011), we determine the factor structure of the multilevel DFM by analysing the pairwise correlations between the factors extracted from each subset of variables separately

Tests of common stochastic trends: Nyblom and Harvey (2000)

4 Temperature intervals: Empirical characteristics

In this section, we describe the data used in this paper as well as their main empirical characteristics.

4.1 The data

One very popular data base for temperature related variables is the Climate Research Unit gridded Time Series (CRU TS) maintained by the university of West Anglia, which is corrected to avoid inhomogeneities; see Mitchell and Jones (2005) and Harris *et al.*

[6] A similar analysis can be carried out for the system of log-ranges.

[7] Each center is deseasonalized using the seasonal component estimated at each location separatelly.

Figure 1: The Iberian Peninsula and Mediterranean islands belonging to Spain with locations where minimum and maximum temperatures are observed marked with blue bullets. The red bullets represent the locations of the main cities in Spain and Portugal, which are the capital of their corresponding provinces.

(2020) for descriptions, Chang *et al.* (2020) for a recent application using this data base and Wijngaard, Klein, Tauk and Können (2003) for a discussion about homogeneity in European temperature series.[8] Intervals of minimum (y_t^{min}) and maximum (y_t^{max}) temperatures (measured in centigrades) are observed monthly from January 1930 to December 2020 ($T = 1092$) in 68 locations in Spain.[9] Figure 1 represents the Iberian Peninsula as well as some islands in the Mediterranean sea belonging Spain and the locations selected for the analysis.

To analyse the main empirical characteristics of the temperature intervals observed in the Iberian Peninsula over the last and present centuries, we select four particular locations, which represent four different climates. The first location selected is Barcelona, a highly populated city situated at the Spanish Mediterranean coast, which obviously

[8]https://sites.uea.ac.uk/cru/data

[9]The minimum and maximum temperatures are monthly means of the individual daily minimum and maximum temperatures. They are not the overall minimum or maximum temperatures recorded each month. Furthermore, we have not considered temperatures in some locations in the Atlantic Ocean because they were rather irregular. Similarly, we found some irregularities in data recorded before 1930. Alternatively, one can use the database E-OBS provided by the European Climate Assessment under the Copernicus project of the European Commission with daily observations since 1950; see, for example, Meng and Taylor (2022) for an application using the E-OBS data set, which can be found at https://cds.climate.copernicus.eu/cdsap#!/dataset/insitu-gridded-observations-europe?tab=overview. However, the E-OBS data base may have issues related with inhomogeneity.

has a Mediterranean climate. The second location is Coruña, a small city laid at the Atlantic Northwest Spanish coast, with an Atlantic climate. The third location considered is Madrid, the largest city in Spain, laid in the center of the Iberian peninsula, with a continental climate. Finally, we consider minimum and maximum temperatures in Seville, in the south of Spain, which has the hottest summer in continental Europe among all cities with a population over 100,000 people; see Figure **??** for a map of the Iberian Peninsula and the localization of the four cities considered.[10]

4.2 Descriptive statistics of minimum/maximum temperature

Next, we describe the main statistical characteristics of minimum and maximum temperatures in the four selected locations in Spain, which are plotted at panels (a) and (b) of Figure 2, respectively. Due to the strong seasonal pattern in monthly minimum and maximum temperature, they are plotted using seasonal polar plots instead of the more popular time plots.[11] First, looking at the minimum temperature plotted in panel (a) of Figure 2, we can conclude that the seasonal patterns observed in Barcelona and Seville are very similar, having the largest seasonal variations. The smallest seasonal variations are observed in Coruña. Second, Figure **??** shows that, as expected, the annual variations of minimum temperatures are larger in the two coastal cities (Barcelona and Coruña) than in the cities located in the interior of the Iberian Peninsula (Madrid and Seville); see also the sample standard deviations of the annual variations reported in Table 1. Moreover, Figure **??** also suggests the possibility of climate change in the four locations considered with minimum temperatures being larger in more recent years than at the beginning of the 20th Century. Similar conclusions are obtained when looking at the polar plots corresponding to maximum temperatures plotted in Figure **??**.

Note that, even if the interest is on modelling IVTS of minimum/maximum temperature, as mentioned above, they cannot be modelled directly as a IVTS without imposing restrictions to avoid their potential crossing at particular moments of time. Consequently,

[10] Meng and Taylor (2022) also consider minimum and maximum temperatures in Madrid and Seville. Instead of analysing Barcelona and Coruña, they consider Cáceres and Albacete. Furthermore, note that they consider daily data, for a shorter period from 1951 to 2015.

[11] The programs needed to obtain the empirical results in this paper has been developed by the first author in R.

we also describe the main statistical properties of the center and log-range temperature, $C_t = \frac{y_t^{max}+y_t^{min}}{2}$ and $R_t = ln(y_t^{max} - y_t^{min})$, respectively; see panels (c) and (d) of Figure 2. The main conclusions for center temperature are similar to those described above for minimum/maximum temperatures. With respect to the log-range temperatures, we can observe that the patterns in the four locations are rather different. First, note that Figure 2b suggests periodic heteroscedasticity with the variance of the shocks being larger in winter than in summer months; see Dupuis (2014) for the same conclusion when looking at minimum temperatures in Southwestern US and Meng and Taylor (2022) for minimum and maximum temperatures in the four cities in Spain mentioned above. Also note that this pattern is more pronounced in the cities located in the interior of the Iberian Peninsula than in those at the coast. With respect to Coruña, the dispersion is smaller than in the rest of the locations but with a very large variability during the years analysed. Finally, the dispersion has decreased in time in Barcelona while, in the other three cities, it seems to increase over the years.

Figure 2: Seasonal polar plots of center and log-range temperature in Barcelona, Coruña, Madrid and Seville.

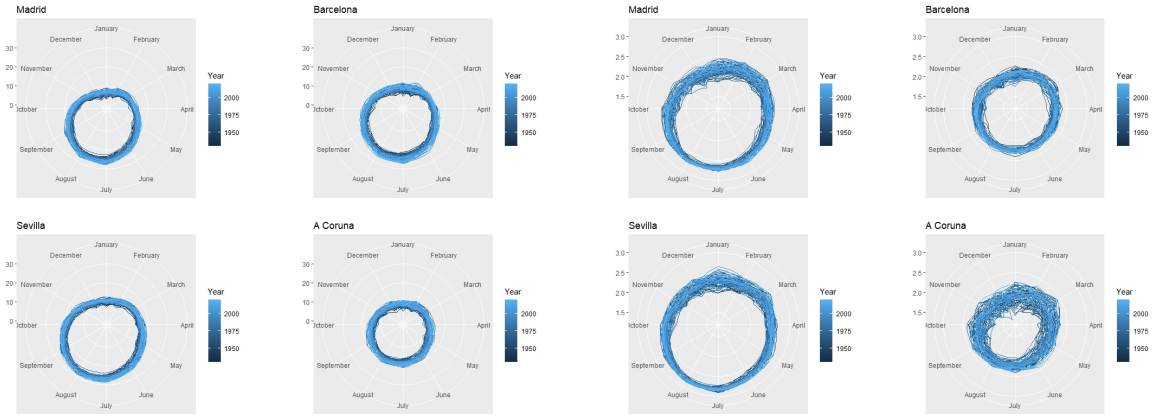

(a) Center (b) Log-range

As mentioned, Figure 2 suggests the presence of possible trends and strong seasonal patterns, some of which may have changed over the last century. Consequently, we analyse the stationarity of the minimum and maximum temperature, as well as of their centres and log-ranges. Table **??** reports the p-values of the Augmented-Dickey-Fuller (ADF) for a unit root at the zero frequency in a model with deterministic trend and seasonal dummies (Fuller, 1976, Dickey and Fuller, 1979, McKinnon, 1991, and Cheung and Lai,

1995) together with those of the test for seasonal unit roots proposed by Dickey, Hasza and Fuller (1984) in a model with seasonal dummies, both implemented to minimum and maximum temperatures at each location. In both cases, the number of lags is 12. It is important to note that the results in Ghysels, Lee and Noh (1994) show the validity of the ADF test for a unit root at the zero frequency in the presence of seasonal dependence as far as the appropriate autoregressive correction terms are augmented to the model.

Table **??** shows that, while the null hypothesis of a unit root at the zero frequency is always rejected, a seasonal unit root is never rejected.[12] There is an ongoing controversy on the relative merits of various alternative unit root and cointegration tests with results potentially different depending on the particular tests used; see, for example, Diebold and Sehadji (1996) and Rao (2010) and the references therein. Kaufmann, Kauppi and Stock (2010) and Kaufmann *et al.* (2013) also discuss about conflicting results on the characteristics of the trends when analysing temperature.

Table 1 reports several descriptive statistics of the annual differences of the center and log-range at each of the four locations. In particular, it reports the sample mean, standard deviation, skewness and kurtosis, the last two together with their p-values obtained according to the results of Bai and Ng (2005). Table 1 also reports the p-values of the Bai and Ng (2005) test for normality in the presence of temporally correlated data and of the Box-Pierce test for joint serial uncorrelation of the first 12 lags.

Figure 3 plots the pairwise correlations among the centers and log-ranges of temperature at all 68 locations in the Iberian Peninsula. it suggests that, at each location, the center temperature and its log-range are not correlated.

As also observed in Figure 2, the log-range variability is larger in Coruña. Furthermore, the log-range series show excess kurtosis.

The polar plots in Figure 2 and the sample moments in Table 1 illustrate climate heterogeneity within Spain. However, some of the patterns can be common at the four locations considered.

Finally, we analyse the presence of clusters among the centers and among the log-

[12]Note that using the HEGY test proposed by Hylleberg *et al.* (1990), with trend a seasonal dummies under the null, the seasonal unit root is always rejected. These results are available upon request. In any case, one should be careful about the results of the HEGY test; see, for example, the Monte Carlo results by Rodrigues and Osborn (2010).

Figure 3: Map of correlations between the centers and the log-ranges in the 68 locations in the Iberian Peninsula.

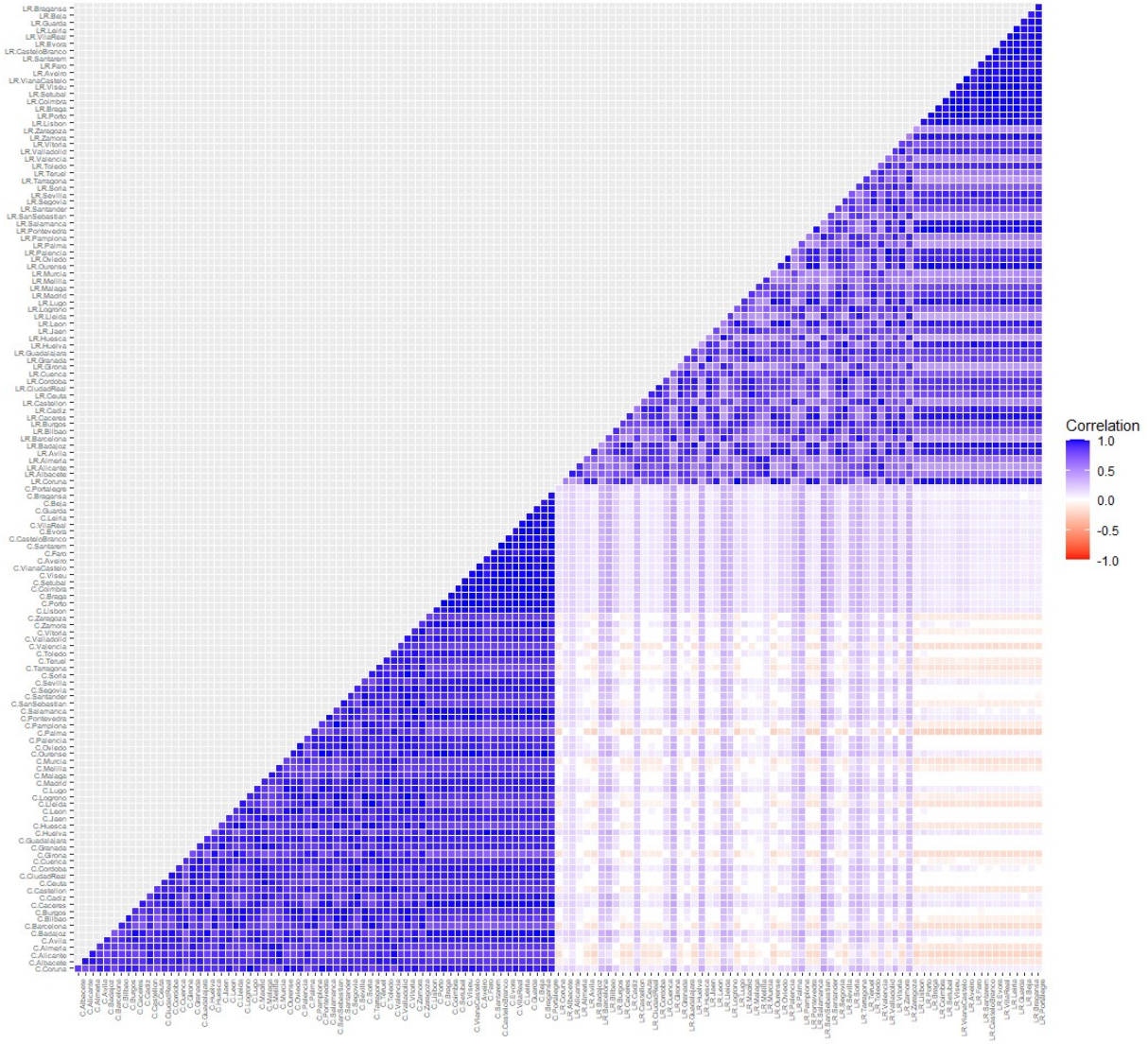

Table 1: Descriptive statistics of annual differences of center and log-range temperature: sample mean (Mean), standard deviation (St. dev.), skewness and kurtosis together with the corresponding p-values of the Bai and Ng () tests of the last two quantities. p-values of the normality test (BN) and of the Box-Pierce test for 12 lags (Q(12)) are also reported.

	Barcelona	Coruña	Madrid	Seville	Barcelona	Coruña	Madrid	Seville
	Center				Log-range			
Mean	0.02	0.02	0.02	0.02	0.00	0.00	0.00	0.00
St. dev.	1.62	1.52	1.50	1.42	0.10	0.20	0.12	0.11
Skewness	0.01	0.02	0.09	0.01	-0.05	-0.10	-0.26	-0.16
	(0.12)	(0.42)	(0.12)	(0.46)	(0.74)	(0.87)	(0.97)	(0.90)
Kurtosis	3.13	2.85	2.87	2.71	3.32	3.55	4.54	4.33
	(0.27)	(0.79)	(0.77)	(0.97)	(0.12)	(0.02)	(0.00)	(0.00)
BN	0.48	0.56	0.17	0.04	0.16	0.00	0.00	0.00
Q(12)	0.00	0.00	0.00	0.00	0.00	0.00	0.00	0.00

Figure 4: Correlation maps of center temperatures (left) and map of the Iberian Peninsula with the resulting clustes (right).

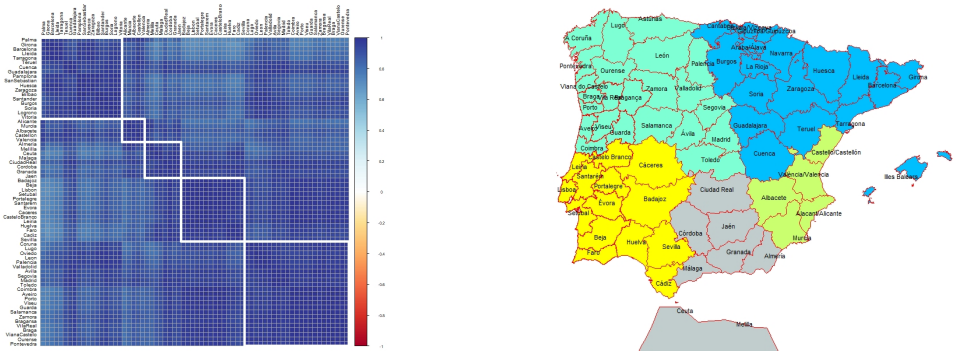

range temperatures. Figure **??** plot the correlation maps for each of them. Using the complete linkage method for hierarchical clustering, which defines the distance between two clusters as the maximum distance between their components, we can identify 5 clusters in the center temperature and 3 in the log-ranges.

Figure 5: Correlation maps of log-range temperatures (left) and map of the Iberian Peninsula with the resulting clustes (right).

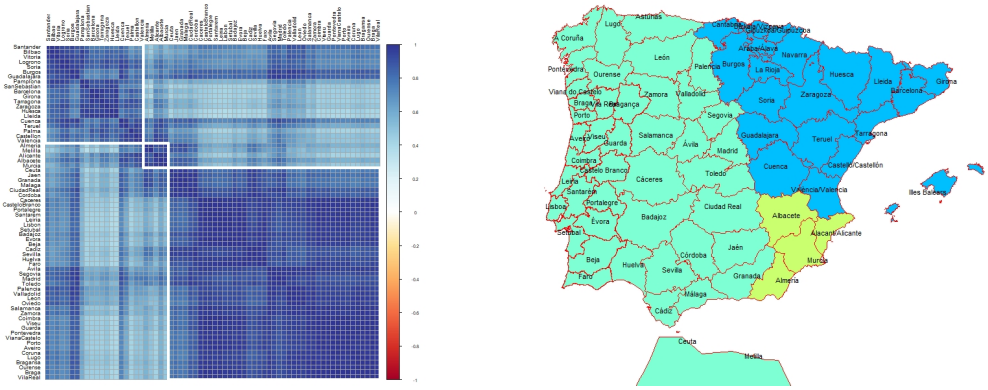

5 Empirical modelling of center and log-range temperature at selected locations in the Iberian Peninsula

In this section, we model the system of center/log-range temperature at four selected locations in the Iberian Peninsula, namely, Barcelona, Coruña, Madrid and Seville.

5.1 Barcelona

Consider first the system of center and log-range temperature observed at Barcelona. The results of fitting model (1a) are reported in the on-line Appendix and show that the shocks of the trend, seasonal and irregular components of the center and log-range are uncorrelated.[13] Consequently, we fit separate DF-BSM to center and log-range.

The estimated parameters of model (1a) are reported in Table 2.[14] We can observe that the trend of the center temperature is represented by an integrated random walk with $\hat{\sigma}^2_\eta$ being approximately zero, implying a smooth evolution, while the trend of the log-range has a constant slope equal to zero, implying that μ_t is a random walk. Figure 22 plots the estimated trends of center and log-range temperature in Barcelona together with

[13] All calculations are carried out by the R programming environment using the free KFAS library developed by Helske (2017).

[14] Note that, based on previous analysis not reported to save space, the seasonal variances of the last five frequencies are assumed to be equal.

their 95% confidence intervals obtained using the MSEs delivered by the Kalman filter. We can observe an increasing trend of the center temperature over the last 90 years with changes in the slope. The center temperature at Barcelona starts around $15°C$ in 1930 while the estimated underlying trend in December 2020 is $17.298°C$. Note that even if we take into account the uncertainty in the estimated trend, the increase of 2 degrees in the center temperature over the last 90 years is clearly significant. With respect to the slope of the trend, we can observe that between 1950 and 1980, the slope was approximately zero. However, since the 80's, we observe an acceleration of the slope of the trend, which stops during the first decade of the XXI century. This dessaceleration is in concordance with the hiatus of average temperature found by Schmidt, Shindell and Tsigaridis (2014), Pretis, Mann and Kaufmann (2015), Medhaug *et al.* (2017) and Miller and Nam (2020), among others. However, the trend of center temperature plotted in Figure 22 shows a recent acceleration since the second decade of the XXI Century. The estimated slope of the trend in December 2020 is 0.004.

Looking at the estimated trend for the log-range temperature in Barcelona, we can observe a level that evolves randomly over time. Note that the fact that the level of log-range is non-stationary, implies that minimum and maximum temperatures are not cointegrated.

When looking at the results reported in table 2 for the seasonal component, the first frequency also shows a smooth temporal evolution over the observed period. Figure 22, which plots the estimated seasonal component for the center temperature, shows a very smooth evolution with the seasonal components being slightly stronger than before; see alos the results for the other three cities considered en Figures 15, 13.

Finally, to assess the adequacy of the specification, Figure 23 plots the QQ plot and estimated autocorrelations of the standardized residuals. Not significant deviation from the normality hypothesis and 21. Significant first order autocorrelations with the autocorrelations being around 0.2 for the center and 0.1 for the log-range. The specification seems to be adequate.

Figure 6: Estimated trend (top row) together with 95% confidence intervals, seasonal (middle row) and irregular (bottom row) of center (left column) and log-range (right column) temperature in Barcelona.

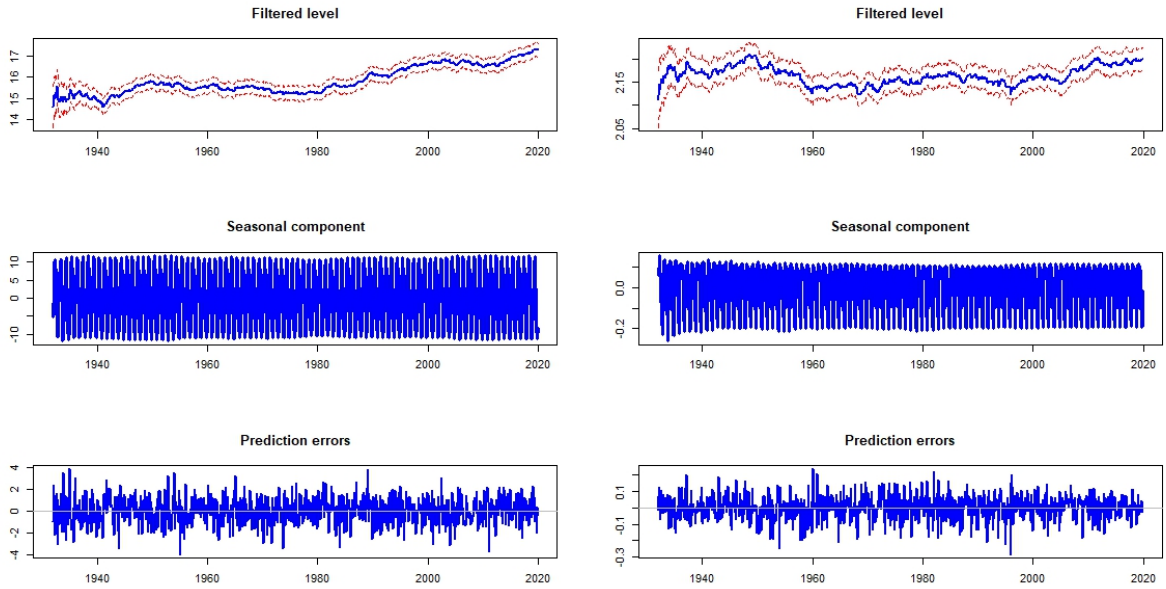

Figure 7: Estimated trend (top row) together with 95% confidence intervals, seasonal (middle row) and irregular (bottom row) of center (left column) and log-range (right column) temperature in Coruña.

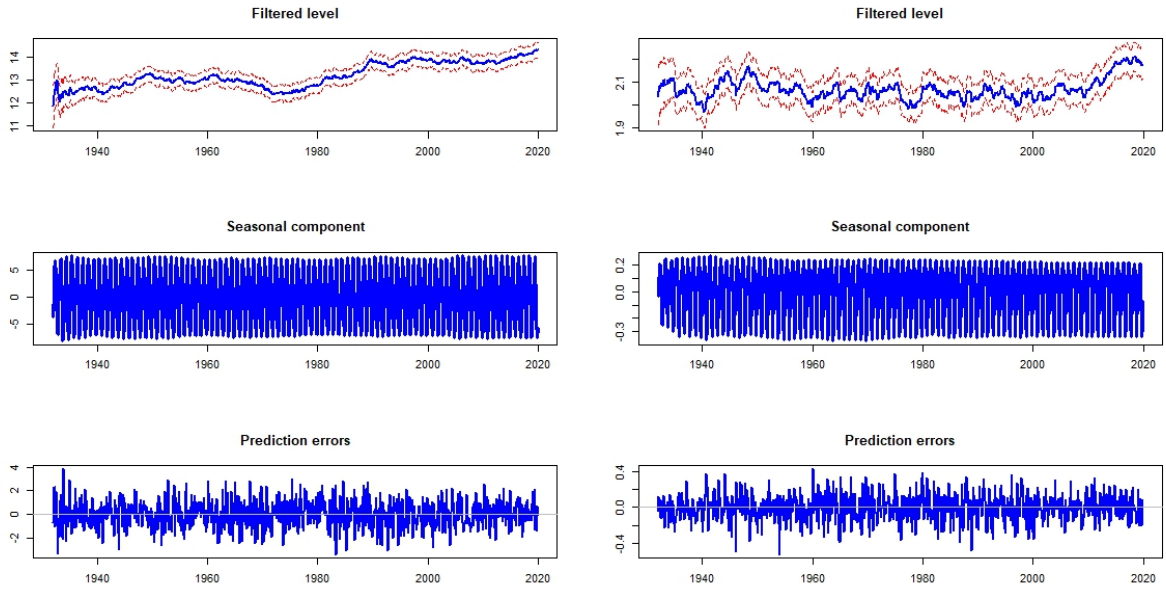

Figure 8: Estimated trend (top row) together with 95% confidence intervals, seasonal (middle row) and irregular (bottom row) of center (left column) and log-range (right column) temperature in Madrid.

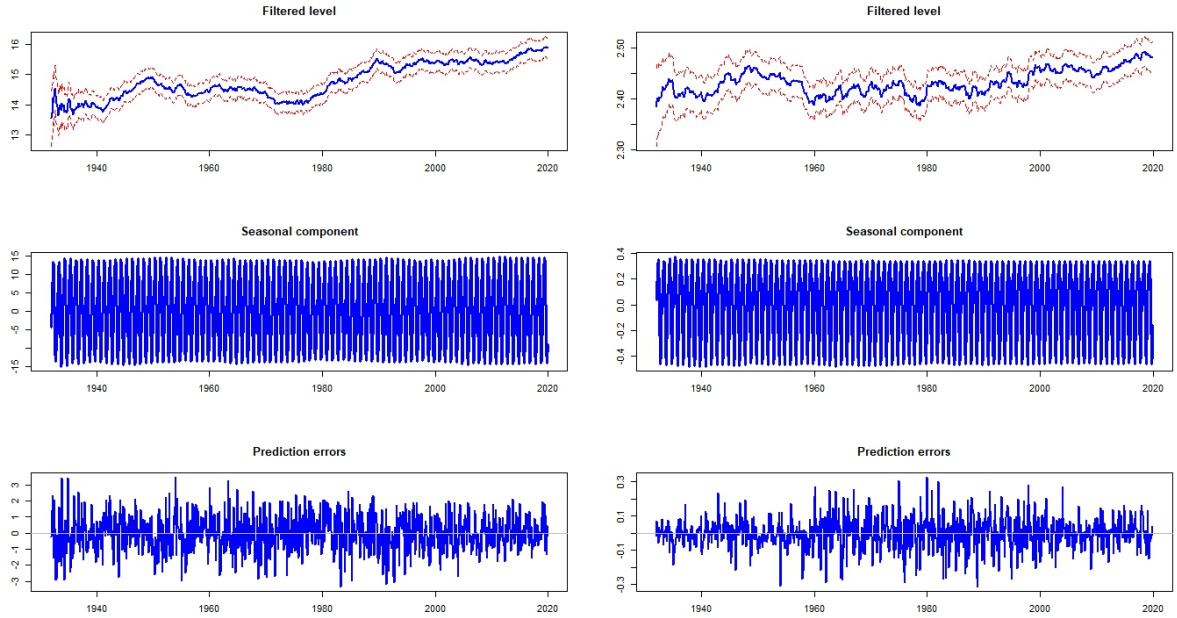

Figure 9: Estimated trend (top row) together with 95% confidence intervals, seasonal (middle row) and irregular (bottom row) of center (left column) and log-range (right column) temperature in Seville.

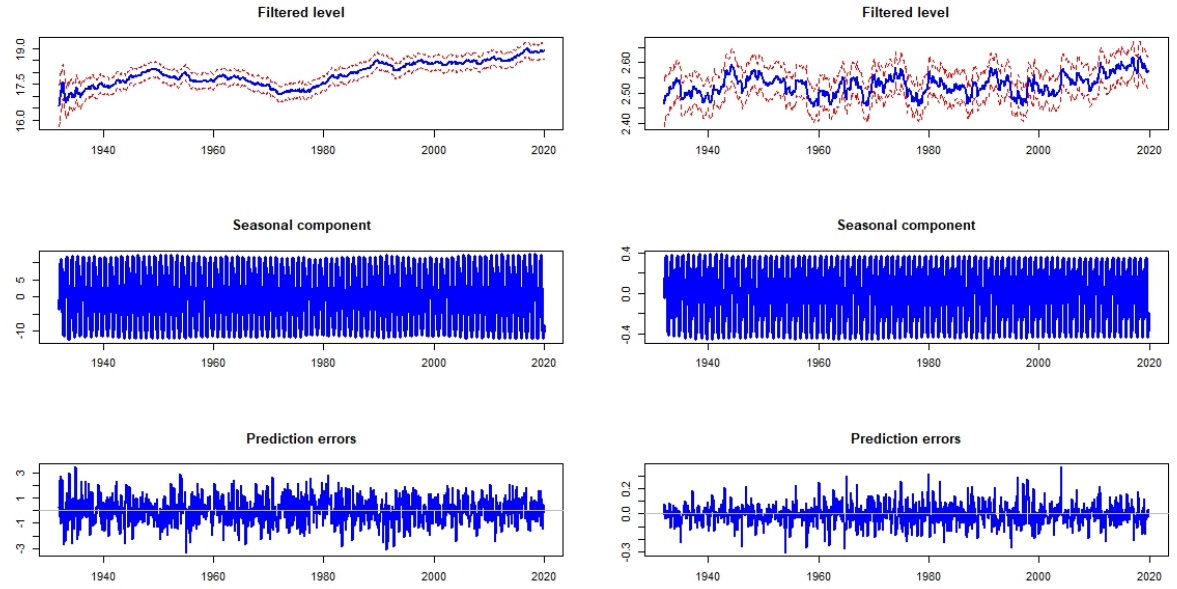

Table 2: Estimation results of separate state space models fitted to center and log-range temperature in four locations in the Iberian Peninsula: i) Estimated variances together with statistics of tests for deterministic components: $H_{0I} : \sigma_{\omega}^{2(I)} = 0$ and $H_{0II} : \sigma_{\omega}^{2(II)} = 0$; ii) Estimated components at the end of the sample period together with standard deviations in parenthesis.

	Center	Log-range	Center	Log-range
	Barcelona		Coruña	
σ_{ε}^2	1.264	0.004	1.141	0.018
σ_{η}^2	1.14×10^{-16}	4.20×10^{-6}	1.50×10^{-16}	5.12×10^{-5}
σ_{ζ}^2	7.85×10^{-8}	1.28×10^{-33}	1.24×10^{-7}	1.62×10^{-33}
$\sigma_{\omega}^{2(I)}$	3.2×10^{-4}	7.53×10^{-28}	3.5×10^{-4}	9.22×10^{-28}
H_{0I}	0.289	1.345***	0.151	0.798***
$\sigma_{\omega}^{2(II)}$	6.6×10^{-25}	6.26×10^{-168}	9.8×10^{-25}	2.11×10^{-167}
H_{0II}	3.616***	1.373	2.292*	2.762**
μ_T	17.294	2.198	14.301	2.176
	(0.167)		(0.170)	
β_T	0.004	3.15×10^{-5}	0.004	0.0001
	(0.003)		(0.003)	
	Madrid		Seville	
σ_{ε}^2	1.111	0.007	1.001	0.006
σ_{η}^2	1.52×10^{-16}	5.84×10^{-6}	2.03×10^{-16}	6.31×10^{-5}
σ_{ζ}^2	1.13×10^{-7}	1.41×10^{-33}	1.10×10^{-7}	1.36×10^{-33}
$\sigma_{\omega}^{2(I)}$	6.3×10^{-4}	8.14×10^{-28}	7.58×10^{-4}	7.89×10^{-28}
H_{0I}	0.171	0.618*	0.112	1.479***
$\sigma_{\omega}^{2(II)}$	9.81×10^{-25}	1.00×10^{-167}	1.45×10^{-24}	8.27×10^{-164}
H_{0II}	2.690*	1.305	2.326**	3.029***
μ_T	15.889	2.483	18.896	2.572
	(0.167)		(0.160)	
β_T	0.003	0.0001	0.002	0.0001
	(0.003)		(0.003)	

*: significant at 10% level; **: significat at 5% level; *** significant at 1% level.

6 Some conclusions

We observe that the shapr of the trends and volatilities of maximum and minimum temperatures can be different in different locations of the Iberian Peninsula. The trends are stochastic with positive slopes.

References

[1] Ahn, H., Y. Kim and Y. Chen (2012), An interval Kalman filtering with minimal conservatism, *Applied Mathematics and Computation*, 218(18), 9563-9570.

[2] Bai, J. and S. Ng (2005), Tests for skewness, kurtosis, and Normality for time series data, *Journal of Business & Economic Statistics*, 23(1), 49-60.

[3] Baillie, R.T. and S.K. Chung (2002), Modeling and forecasting from trend-stationary long memory models with applications to climatology, *Journal of Forecasting*, 18(2), 215-226.

[4] Banbura et al. (2011), Nowcasting, in *Oxford Handbook of Economic Forecasting*.

[5] Barbosa, S.M., M.G. Scotto and A. Alonso (2011), Summarizing changes in air temperature over Central Europe by quantile regression and clustering, *Natural Hazards and Earth System Sciences*, 11, 3227-3233.

[6] Banerjee, A., J.J. Dolado and R. Mestre (1998), Error-correction mechanism tests for cointegration in a single-equation framework, *Journal of Time Series Analysis*, 19(3), 267-283.

[7] Barnett, M., W. Brock and L.P. Hansen (2021), Climate change uncertainty spillover in the macroeconomy, *NBER Macroeconomics*, 36.

[8] Beyaztas, B.H. (2021), Construction of multi-step forecast regions of VAR processes using ordered block bootstrap, *Communications in Statistics-Simulation and Computation*, 50(7), 2107-2125.

[9] Binelli, C., M. Loveless and B.F. Schaffner (in press), Explaining perceptions of climate change in the US, *Political Research Quarterly*.

[10] Bloomfield, P. (1992), Trends in global temperature, *Climatic Change*, 21, 1-16.

[11] Bolton, P., M. Despres, L.A. Pereira da Silva, F. Samama and R. Svartzman (2020), *The Green Swan: Central Banking and Financial Stability in the Age of Climate Change*, BIS Books, Bank of International Settlements.

[12] Breitung, J. and S. Eickmeier (2016), Analyzing international business and financial cycles using multi-level factor models: A comparison of alternative approaches, in.... *Dynamic Factor Models*.

[13] Busetti, F. (2006), Test of seasonal integration and cointegration in multivariate unobserved component models, *Journal of Applied Econometrics*, 21, 419-438.

[14] Busetti, F. and A.C. Harvey (2003), Seasonality tests, *Journal of Business & Economic Statistics*, 21(3), 420-436.

[15] Busetti, F. and A.C. harvey (2008), Testing for trend, *Econometric Theory*, 24, 72-87.

[16] Campbell, S.D. and F.X. Diebold (2005), Weather forecasting for weather derivatives, *Journal of the American Statistical Association*, 100(469), 6-16.

[17] Caporin, M., A. Ranaldo and P. Santucci de Magistris (2013), On the predictability of stock prices: A case for high and low prices, *Journal of Banking and Finance*, 37(12), 5132-5146.

[18] Chang, Y., R.K. Kaufmann, C.S. Kim, J.I. Millers, J.Y. Park and S. Park (2020), Evaluating trends in time series of distributions: A spatial fingerprint of human effects on climate, *Journal of Econometrics*, 214(1), 274-294.

[19] Chen, L. J. Gao and F. Vahid (in press), Global temperatures and greenhouse gases: A common features approach, *Journal of Econometrics*.

[20] Chen, G., J. Wang and L.S. Shieh (1997), Interval Kalman filtering, *IEEE Transactions on Aerospace and Electronic Systems*, 33(1), 250-258.

[21] Cheung, Y. (2007), An empirical model of daily highs and lows, *International Journal of Finance and Economics*, 12, 1-20.

[22] Cheung, Y.L., Y.W. Cheung and A.T. Wan (2009), A high-low model of daily stock price ranges, *Journal of Forecasting*, 28(2), 103-119.

[23] Cheung, Y.W. and K.S. Lai (1995), Lag order and critical values of the augmented Dikey-Fuller test, *Journal of Business & Economic Statistics*, 13(3), 277-280.

[24] Chou, R., 2005, Forecasting financial volatilities with extreme values: the conditional autoregressive (CARR) model, *Journal of Money, Credit, and Banking*, 37, 561-582.

[25] Coggin, T.D. (2012), Using econometric methods to test for trends in the HadCRUT3 global and hemispheric data, *International Journal of Climatology*, 32(2), 315-320.

[26] Cubadda, G. (1999), Common cycles in seasonal non-stationary time series, *Journal of Applied Econometrics*, 14(3), 273-291.

[27] Darné, O. (2004), Seasonal cointegration for monthly data, *Economics Letters*, 82(3), 349-356.

[28] Delle Chiae, Ferrara, Giannone (2022), *Journal of Applied Econometrics*, 37, 461-476.

[29] Deng, Q. and Z. Fu (2019), Comparison of methods for extracting annual cycle with changing amplitude in climate series, *Climate Dynamics*, 52, 5059-5070.

[30] Dickey, D.A. and W.A. Fuller (1979), Distribution of the estimators for autoregressive time series with unit roots, *Journal of the American Statistical Association*, 74, 427-431.

[31] Dickey, D.A., D.P. Hasza and W.A. Fuller (1984), Testing for unit roots in seasonal time series, *Journal of the American Statistical Association*, 79(386), 355-367.

[32] Diebold, F.X. and G.D. Rudebusch (2022a), On the evolution of U.S. temperature dynamics, in Chudik, A., C. Hsiao and A. Timmermann (eds.), *Essays in Honor of Hashem Pesaran: Prediction and Macro Modeling*, Advances in Econometrics, 43A, Emerald Publishing Limited.
bibitemDiebold, F.X. and G.D. Rudebusch (2022b), Probability assessments of an ice-free Arctic: Comparing statistical and climate model projections, *Journal of Econometrics*, 231(2), 520-534.

[33] Diebold, F.X. and A.S. Senhadji (1996), The uncertain unit root in real GNP: Comment, *American Economic Review*, 86(5), 1291-1298.

[34] Dupuis, D.J. (2012), Modelling waves of extreme temperature: the changing tails of four cities, *Journal of the American Statistical Association*, 107(497), 24-39.

[35] Dupuis, D.J. (2014), A model for nighttime minimum temperatures, *Journal of Climate*, 27(19), 7207-7229.

[36] Durbin, J. and S.J. Koopman (2012), *Time Series Analysis by State Space Methods*, 2nd. ed., Oxford University Press, New York.

[37] Estrada, F. and P. Perron (2021), Disentangling the trend in the warming of urban areas into global and local factors, *Annals of the New York Academy of Sciences*, 1504, 230-246.

[38] Estrada, F., C. Gay and A. Sánchez (2010), A reply to "Does temperature contain a stochastic trend? Evaluating conflicting statistical results" by Kaufmann *et al.*, *Climatic Change*, 101(3), 407-414.

[39] Estrada, F., D. Kim and P. Perron (2021), Spatial variations in the warming trend and the transition to more severe weather in midlatitudes, *Scientific Reports*, 11(145).

[40] Estrada, F. P. Perron and B. Martínez-López (2013), Statistically derived contributions of diverse human influences to twentieth-century temperature changes, *Nature Geoscience*, 6(12), 1050-1055.

[41] Fatichi, S., S.M. Barbosa, E. Caporali and M.E. Silva (2009), Deterministic versus stochastic trends: Detection and challenges, *Journal of Geophysical Research*, 114, D18121.

[42] Fresoli, D., E. Ruiz and L. Pascual (2015), Bootstrap multi-step forecasts of non-Gaussian VAR models, *International Journal of Forecasting*, 31(3), 834-848.

[43] Friedrich, M., S. Smeekes and J.-P. Urbain (2020), Autoregressive wild bootstrap inference for nonparametric trends, *Journal of Econometrics*, 214(1), 81-109.

[44] Friedrich, M., E. Beutner, H. Reuvers, S. Smeekes, J.-P. Urbain, W. Bader, B. Franco, B. Lejeune and E. Mahieu (2020), A statistical analysis of time trends in atmospheric ethane, *Climatic Change*, 162, 105-125.

[45] Fuller, W.A. (1976), *Introduction to Statistical Time Series*, John Wiley, New York.

[46] Gadea Rivas, M.D. and J. Gonzalo (2020), Trends in distributional characteristics: Existence of global warming, *Journal of Econometrics*, 214, 153-174.

[47] Gadea Rivas, M.D. and J. Gonzalo (2022), A tale of three cities: climate heterogeneity, *SERIEs*, 13, 475-511.

[48] Gao, J. and K. Hawthorne (2006), Semiparametric estimation and testing of the trend of temperature series, *Econometrics Journal*, 9(2), 332-355.

[49] Gay, G.C., F. Estrada and A. Sánchez (2009), Global and hemispheric temperatures revisited, *Climatic Change*, 94(3-4), 333-349.

[50] Ghysels, E. H.S. Lee and J. Noh (1994), Testing for unit roots in seasonal time series: Some theoretical extensions and Monte Carlo investigation, *Journal of Econometrics*, 62(2), 415-442.

[51] Gil-Alana, L.A. (2005), Statistical modelling of the temperatures in the Northern hemisphere using fractional integration techniques, *Journal of Climate*, 18(24), 5357-5369.

[52] González-Rivera, G., Y. Luo and E. Ruiz (2020), Prediction regions for interval-valued time series, *Journal of Applied Econometrics*, 35(4), 373-390.

[53] Good, S., G. Corlett, J. Remedios, E. Noyes and D. Llewellyn-Jones (2007), The global trend in sea surface temperature from 20 years of advanced very high resolution radiometer data, *Journal of Climate*, 20, 1255-1264.

[54] Harris, I., T.J. Osborn, P. Jones and D. Lister (2020), Version 4 of the CRUTS monthly high-resolution gridded multivariate climate dataset, *Scientific Data*, 7(109).

[55] Harvey, A.C. (1997), Trends, cycles and autoregression, *Economic Journal*, 107, 192-201.

[56] Harvey, A.C. (1989), *Forecasting, Structural Time Series Models and the Kalman Filter*, Cambridge University Press, Cambridge.

[57] Harvey, A.C. (2001), Testing in unobserved components models, *Journal of Forecasting*, 20(1), 1-19.

[58] Harvey, A.C. and A. Jaeger (1993), Detrending, stylized facts and the business cycle, *Journal of Applied Econometrics*, 8, 231-247.

[59] Hausfather, Z., M.J. Menne, C.N. Williams, T. Masters, R. Broberg and D. Jones (2013), Quantifying the effect of urbanization in U.S. historical climatology network temperature records, *Journal of Geophysical Research: Atmospheres*, 118, 481-494.

[60] He, Y., A. Han, Y. Hong, Y. Sun and S. Wang (2021), Forecasting crude oil price intervals and return volatility via autoregressive conditional interval models, *Econometric Reviews*, 40(6), 584-606.

[61] He, C., J. Kang, T. Teräsvirta and S. Zhang (2019), The shifting seasonal mean autoregressive model and seasonality in the Central England monthly temperature series, 1772-2016, *Econometrics and Statistics*, 12, 1-24.

[62] He, C., J. Kang, T. Teräsvirta and S. Zhang (2021), Comparing long monthly Chinese and selected European temperature series using Vector Seasonal Shifting Mean and Covariance Autoregressive model, *Energy Economics*, 105171.

[63] Helske, J. (2017), KFAS: Exponential family state space models in R, *Journal of Statistical Software*, 78(10).

[64] Hindrayanto, I., J.A.D. Aston, S.J. Koopman and M. Ooms (2013), Modeling trigonometric seasonal components for monthly economic time series, *Applied Economics*, 45(21), 3024-3034.

[65] Holt, M.T. and T. Teräsvirta (2020), Global hemispheric temperatures and coshifting: A vector shifting-mean autoregressive analysis, *Journal of Econometrics*, 214(1), 198-215.

[66] Hsiang, S. and R.E. Koop (2018), An economist's guide to climate change science, *Journal of Economic Perspectives*, 32, 3-32.

[67] Hylleberg, S., R.F. Engle, C.W.J. Granger and B.S. Soo (1990), Seasonal integration and cointegration, *Journal of Econometrics*, 44(1-2), 215-238.

[68] IPCC (2014), AR5 Synthesis report: Climate Change 2014. Contribution of working groups I, II and III to the Fifth Assessment Report of the Intergovernmental Panel on Climate Change. [Core Writing Team, R.K. Pachauri and L.A. Meyer (eds.)]. IPCC, Geneva, Switzerland.

[69] IPCC (2022), AR6 Synthesis report: Climate Change 2022. Contribution of working groups I, II and III to the Sixth Assessment Report of the Intergovernmental Panel on Climate Change. [Core Writing Team, ...(eds.)]. IPCC, Geneva, Switzerland.

[70] Katz, R.W. and B.G. Brown (1992), Extreme events in a changing climate: Variability is more important than averages, *Climatic Change*, 21, 289-302.

[71] Kaufmann, R.K. and D.I. Stern (1997), Evidence from human influence on climate from hemispheric temperature relations, *Nature*, 388(6637), 39-44.

[72] Kaufmann, R.K., H. Kauppi and J.H. Stock (2010), Does temperature contain a stochastic trend? Evaluating conflicting statistical results, *Climatic Change*, 101, 395-405.

[73] Kaufmann, R.K., H. Kauppi, M.L. Mann and J.H. Stock (2013), Does temperature contain a stochastic trend: linking statistical results to physical mechanisms, *Climatic Change*, 118, 729-743.

[74] Kaufmann, R.K., M.L. Mann, S. Gopal, J.A. Liederman, P.D. Howe, F. Pretis, X. Tang and M. Gilmore (2017), Spatial heterogeneity of climate change as an experimental basis for skepticism, *Proceedings of the National Academy of Sciences, PNAS*, 114(1), 67-71.

[75] Kew, S.F., S.Y. Philip, G. Jan van Oldenborgh, G. van der Schrier, F.E. Otto and R. Vautard (2019), The exceptional summer heat wave in southern Europe 2017, *Bulletin of the American Meteorological Society*, 100(1), S49-S53.

[76] Kim, D., T. Oka, F. Estrada abd P. Perron (2020), Inference related to common breaks in a multivariate system with joined segmented trends with applications to global and hemispheric temperatures, *Journal of Econometrics*, 214, 130-152.

[77] Lee, H., J. Lee and K. Im (2015), More powerful cointegration tests with non-normal errors, *Studies in Nonlinear Dynamics and Econometrics*, 19(4), 397-413.

[78] Maharaj, E.A., P. Brito and P. Teles (2021), A test to compare interval time series, *International Journal of Approximate Reasoning*, 133, 17-29.

[79] Maia, A.L.S. and F.A.T. de Carvalho (2011), Holt's exponential smoothing and neural network models for forecasting interval-valued time series, *International Journal of Forecasting*, 27(3), 740-759.

[80] Mangat, M.K. and E. Reschenhofer (2020), Frequency-domain evidence for climate change, *Econometrics*, 8(3), 28.

[81] McKinnon, J.G. (1996), Numerical distribution functions for unit root and cointegration tests, *Journal of Applied Econometrics*, 11, 601-618.

[82] Megdhaug, L., M.B. Stolpe, E.M. Fisher and R. Knutti (2017), Reconciling controversies about the "global warming hiatus", *Nature*, 545(7652), 41-47.

[83] Meng, X. and J.W. Taylor (2022), Comparing probabilistic forecasts of the daily minimum and maximum temperature, *International Journal of Forecasting*, 38, 267-281.

[84] Miller, J.I. and K. Nam (2020), Dating Hiatuses: a statistical model of the recent slowdown in global warming and the next one, *Earth System Dynamics*, 11, 1123-1132.

[85] Miller, S., K. Chua, J. Coggings and H. Mohtadi (2021), Heat waves, climate change, and economic output, *Journal of European Economic Association*, 19(5), 2658-2694.

[86] Mitchell, T.D. and P.D. Jones (2005), An improved method of constructing a database of monthly climate observations and associated high-resolution grids, *International Journal of Climatology*, 25(6), 693-712.

[87] Nyblom, J. and A.C. Harvey (2000a), Testing against smooth stochastic trends, *Journal of Applied Econometrics*, 16(3), 415-429.

[88] Nyblom, J. and A.C. Harvey (2000b), Tests of common stochastic trends, *Econometric Theory*, 16, 176-199.

[89] Palmer, T. and R. Stevens (2019), The scientific challenge of understanding and estimating climate change, *Proceedings of the National Academy of Sciences*, 116(49), 24390-24395.

[90] Pezzulli, S., D. Stephenson and A. Hannachi (2005), The variability of seasonality, *Journal of Climate*, 18, 71-88.

[91] Phillips, P.C.B. (2005), Challenges of trending time series econometrics, *Mathematics and Computers in Simulation*, 68(5), 401-416.

[92] Phillips, P.C.B. (2010), The mysteries of trend, *Macroeconomic Reviews*, 9(2), 82-89.

[93] Pindyck, R.S. (2013), Climate change policy, what do the models tell us?, *Journal of Economic Literature*, 51(3), 860-872.

[94] Pretis, F. and M. Allen (2013), Breaks in trends, *Nature Geoscience*, 6(12), 992-993.

[95] Pretis, F. and D.F. Hendry (2013), Comment on "Polynomial cointegration tests of anthropogenic impact on global warming" by Beenstock *et al.* (2012)-some hazards in econometric modelling of climate change, *Earth System Dynamics*, 4, 375-384.

[96] Pretis, F., M.L. Mann and R.K. Kaufmann (2015), Testing competing models of the temperature hiatus: assessing the effects of conditioning variables and temproal uncertainties through sample-wide break detection, *Climatic Change*, 131, 705-718.

[97] Proietti, T. and E. Hillebrand (2017), Seasonal changes in central England temperatures, *Journal of the Royal Statistical Society, Series A (Statistics and Society)*, 180(3), 769-791.

[98] Qu, M., J. Wan and X. Hao (2014), Analysis of diurnal air temperature range in the continental United States, *Weather and Climate Extremes*, 4, 86-95.

[99] Rao, B.B. (2010), Deterministic and stochastic trends in time series models: a guide for the applied economist, *Applied Economics*, 42(17), 2193-2202.

[100] Ren, T., W. Zhou and J. Wang (2021), Beyond intensity of urban heat island effect: A continental scale analysis on land surface temperature in major Chinese cities, *Science of The Total Environment*, 791, 148334.

[101] Rodrigues, P.M.M. and D.R. Osborn (2010), Performance of seasonal unit root tests for seasonal data, *Journal of Applied Statistics*, 26(8), 985-1004.

[102] Schmidt, G.A., D.T. Shindell and K. Tsigaridis (2014), Reconciling warming trends, *Nature Geoscience*, 7(3), 158-160.

[103] Schmidt, G.A. et al., 2014, Using paleo-climate comparisons to constrain future projections in CMIP5, *Climate of the Past*, 10, 221-250.

[104] Scotto, M.G., S.M. Barbosa and A.M. Alonso (2011), Extreme value and cluster analysis of European daily temperature series, *Journal of Applied Statistics*, 38(12), 2793-2804.

[105] Seidel, D.J. and J.R. Lanzante (2004), An assessment of three alternatives to linear trends for characterizing global atmospheric temperature changes, *Journal of Geophysical Research: Atmospheres*, 109(D14).

[106] Seong, B., S. Cho, S.K. Ahn and S.Y. Hwang (2008), Effects of the misspecification of cointegrating ranks in seasonal models, *The Korean Journal of Applied Statistics*, 21(5), 783-789.

[107] Stern, D.I. and R.K. Kaufmann (2000), Detecting a global warming signal in hemispheric temperature series: A structural time series analysis, *Climate Change*, 47, 411-438.

[108] Ventosa-Santaulalia, D., D.R. Heres and L.C. Martínez-Hernández (2014), Long-memory and the sea-level temperature relationship: A fractional cointegration approach, *PloS One*, 9(11), e113439.

[109] Vera-Valdés, J.E. (2021), Temperature anomalies. Long-memory and aggregation, *Econometrics*, 9(1), 9.

[110] Visser, H. and J. Molenaar (1995), Trend estimation and regression analysis in climatological time series: An application of structural time series models and the Kalman filter, Journal of Climate, 8(5), 969-979.

[111] Vose, R.S., D.R. Easterling and B. Gleason (2005), Maximum and minimum temperature trends for the globe: An update through 2004, *Geophysical Research Letters*, 32, L23822.

[112] Wang, Z., Y. Jiang, H. Wan, J. Yan and X. Zhang (2021), Toward optimal fingerprint in detection and attribution of changes in climate extremes, *Journal of the American Statistical Association*, 116(533), 1-13.

[113] Wijngaard, J.B., A.M.G. Klein Tauk and G.P. Können (2003), Homogeneity of 20th century European daily temperature and precipitations series, *International Journal of Climatology*, 23, 679-692.

[114] Woodward, W.H. and H.L. Gray (1993), Global warming and the problem of testing for trend in time series data, *Journal of Climate*, 6, 953-962.

[115] Xiong, T., Y. Bao and Z. Hu (2014), Multiple-output support vector regression with a firefly algorithm for interval-valued stock price index forecasting, *Knowledge-Based Systems*, 55, 87-100.

[116] Xiong, T., C. Li and Y. Bao (2017), Interval-valued time series forecasting using a novel hybrid Holt[1] and MSVR model, *Economic Modelling*, 60, 11-23.

[117] Xu, W., Q. Li, X.L. Wang, S. Yao, L. Cao and Y. Feng (2013), Homogenization of Chinese daily surface air temperatures and analysis of trends in the extreme temperature indices, *Journal of Geophysical Research: Atmospheres*, 118(17), 9708-9720.

[118] Zaval, L. E.A. Keenan, E.J. Johnson and E.U. Weber (2014), How warm days increase belief in global warming, *Nature Climate Change*, 4(2), 143-147.

[119] Zhang, D., L. Qian, M. Amin and L. Liwen (2020), A hybrid model considering cointegration for interval-valued pork price forecasting in China, *Journal of Forecasting*, 39, 1324-1341.

[120] Zheng, X. and R.E. Basher (1999), Structural time series models and trend detection in global and regional temperature series, *Journal of Climate*, 12, 2347-2358.

Supplementary Material

A STATE SPACE MODEL

Consider model (1) for the center and log-range temperature. This model can be written in state space form as follows

$$X_t = Z\alpha_t + \varepsilon_t, \tag{A.1a}$$

$$\alpha_t = T\alpha_{t-1} + \eta_t, \tag{A.1b}$$

where $\alpha_t = \left(\mu_{1t}, \mu_{2t}, \beta_{1t}, \beta_{2t}, \gamma_{1t}^{(1)}, \gamma_{2t}^{(1)}, \gamma_{1t}^{*(1)}, \gamma_{2t}^{*(1)}, \gamma_{1t}^{(2)}, \gamma_{2t}^{(2)}, \gamma_{1t}^{*(2)}, \gamma_{2t}^{*(2)} ..., \gamma_{1t}^{(6)}, \gamma_{2t}^{(6)}\right)'$ is the 26×1 vector of unobserved states, the 2×26 observation matrix Z is given by

$$Z = \begin{bmatrix} 1 & 0 & 0 & 0 & -1 & 0 & 0 & 0 & -1 & 0 & 0 & 0 & -1 & 0 & 0 & 0 & -1 & 0 & 0 & 0 & -1 & 0 & 0 & 0 & -1 & 0 \\ 0 & 1 & 0 & 0 & 0 & -1 & 0 & 0 & 0 & -1 & 0 & 0 & 0 & -1 & 0 & 0 & 0 & -1 & 0 & 0 & 0 & -1 & 0 & 0 & 0 & -1 \end{bmatrix}, \tag{A.2}$$

while the 26×26 transition matrix T is given by

$$T = \begin{bmatrix} 1 & 0 & 1 & 0 & 0 & 0 & 0 & 0 & 0 & 0 & 0 & 0 & 0 & \cdots & 0 & 0 \\ 0 & 1 & 0 & 1 & 0 & 0 & 0 & 0 & 0 & 0 & 0 & 0 & 0 & \cdots & 0 & 0 \\ 0 & 0 & 1 & 0 & 0 & 0 & 0 & 0 & 0 & 0 & 0 & 0 & 0 & \cdots & 0 & 0 \\ 0 & 0 & 0 & 1 & 0 & 0 & 0 & 0 & 0 & 0 & 0 & 0 & 0 & \cdots & 0 & 0 \\ 0 & 0 & 0 & 0 & cos\lambda_1 & 0 & sin\lambda_1 & 0 & 0 & 0 & 0 & 0 & 0 & \cdots & 0 & 0 \\ 0 & 0 & 0 & 0 & 0 & cos\lambda_1 & 0 & sin\lambda_1 & 0 & 0 & 0 & 0 & 0 & \cdots & 0 & 0 \\ 0 & 0 & 0 & 0 & -sin\lambda_1 & 0 & cos\lambda_1 & 0 & 0 & 0 & 0 & 0 & 0 & \cdots & 0 & 0 \\ 0 & 0 & 0 & 0 & 0 & -sin\lambda_1 & 0 & cos\lambda_1 & 0 & 0 & 0 & 0 & 0 & \cdots & 0 & 0 \\ 0 & 0 & 0 & 0 & 0 & 0 & 0 & 0 & cos\lambda_2 & 0 & sin\lambda_2 & 0 & 0 & \cdots & 0 & 0 \\ 0 & 0 & 0 & 0 & 0 & 0 & 0 & 0 & 0 & cos\lambda_2 & 0 & sin\lambda_2 & 0 & \cdots & 0 & 0 \\ 0 & 0 & 0 & 0 & 0 & 0 & 0 & 0 & -sin\lambda_2 & 0 & cos\lambda_2 & 0 & 0 & \cdots & 0 & 0 \\ 0 & 0 & 0 & 0 & 0 & 0 & 0 & 0 & 0 & -sin\lambda_2 & 0 & cos\lambda_2 & 0 & \cdots & 0 & 0 \\ \vdots & \vdots & \vdots & \vdots & \vdots & \vdots & \vdots & \vdots & \vdots & \vdots & \vdots & \vdots & \ddots & \vdots & \vdots & \vdots \\ 0 & 0 & 0 & 0 & 0 & 0 & 0 & 0 & 0 & 0 & 0 & 0 & \cdots & cos\lambda_6 & 0 & \\ 0 & 0 & 0 & 0 & 0 & 0 & 0 & 0 & 0 & 0 & 0 & 0 & \cdots & 0 & cos\lambda_6. & \end{bmatrix} \tag{A.3}$$

Finally, the covariance matrix of ε_t is assumed to be constant over time and given by

$$H = \begin{bmatrix} \sigma_{\varepsilon 1}^2 & \sigma_{\varepsilon 12} \\ \sigma_{\varepsilon 12} & \sigma_{\varepsilon 2}^2, \end{bmatrix} \tag{A.4}$$

while the covariance matrix of η_t is given by

$$Q = \begin{bmatrix} \sigma_{\nu 1}^2 & \sigma_{\nu 12} & 0 & 0 & 0 & 0 & 0 & 0 & 0 & 0 & 0 & 0 & \cdots & 0 & 0 \\ \sigma_{\nu 12} & \sigma_{\nu 2}^2 & 0 & 0 & 0 & 0 & 0 & 0 & 0 & 0 & 0 & 0 & \cdots & 0 & 0 \\ 0 & 0 & \sigma_{\zeta 1}^2 & \sigma_{\zeta 12} & 0 & 0 & 0 & 0 & 0 & 0 & 0 & 0 & \cdots & 0 & 0 \\ 0 & 0 & \sigma_{\zeta 12} & \sigma_{\zeta 1}^2 & 0 & 0 & 0 & 0 & 0 & 0 & 0 & 0 & \cdots & 0 & 0 \\ 0 & 0 & 0 & 0 & \sigma_{\omega 1}^2 & \sigma_{\omega 12} & 0 & 0 & 0 & 0 & 0 & 0 & \cdots & 0 & 0 \\ 0 & 0 & 0 & 0 & \sigma_{\omega 12} & \sigma_{\omega 2}^2 & 0 & 0 & 0 & 0 & 0 & 0 & \cdots & 0 & 0 \\ 0 & 0 & 0 & 0 & 0 & 0 & \sigma_{\omega 1}^2 & \sigma_{\omega 12} & 0 & 0 & 0 & 0 & \cdots & 0 & 0 \\ 0 & 0 & 0 & 0 & 0 & 0 & \sigma_{\omega 12} & \sigma_{\omega 2}^2 & 0 & 0 & 0 & 0 & \cdots & 0 & 0 \\ 0 & 0 & 0 & 0 & 0 & 0 & 0 & 0 & \sigma_{\omega 1}^2 & \sigma_{\omega 12} & 0 & 0 & \cdots & 0 & 0 \\ 0 & 0 & 0 & 0 & 0 & 0 & 0 & 0 & \sigma_{\omega 12} & \sigma_{\omega 2}^2 & 0 & 0 & \cdots & 0 & 0 \\ 0 & 0 & 0 & 0 & 0 & 0 & 0 & 0 & 0 & 0 & \sigma_{\omega 1}^2 & \sigma_{\omega 12} & \cdots & 0 & 0 \\ 0 & 0 & 0 & 0 & 0 & 0 & 0 & 0 & 0 & 0 & \sigma_{\omega 12} & \sigma_{\omega 2}^2 & \cdots & 0 & 0 \\ \vdots & \vdots & \vdots & \vdots & \vdots & \vdots & \vdots & \vdots & \vdots & \vdots & \vdots & \vdots & \ddots & \vdots & \vdots \\ 0 & 0 & 0 & 0 & 0 & 0 & 0 & 0 & 0 & 0 & 0 & 0 & \cdots & \sigma_{\omega 1}^2 & \sigma_{\omega 12} \\ 0 & 0 & 0 & 0 & 0 & 0 & 0 & 0 & 0 & 0 & 0 & 0 & \cdots & \sigma_{\omega 12} & \sigma_{\omega 2}^2. \end{bmatrix} \tag{A.5}$$

Figure 10: Estimated trend (top row), seasonal (middle row) and irregular (bottom row) of center (left column) and log-range (right column) temperature in Barcelona.

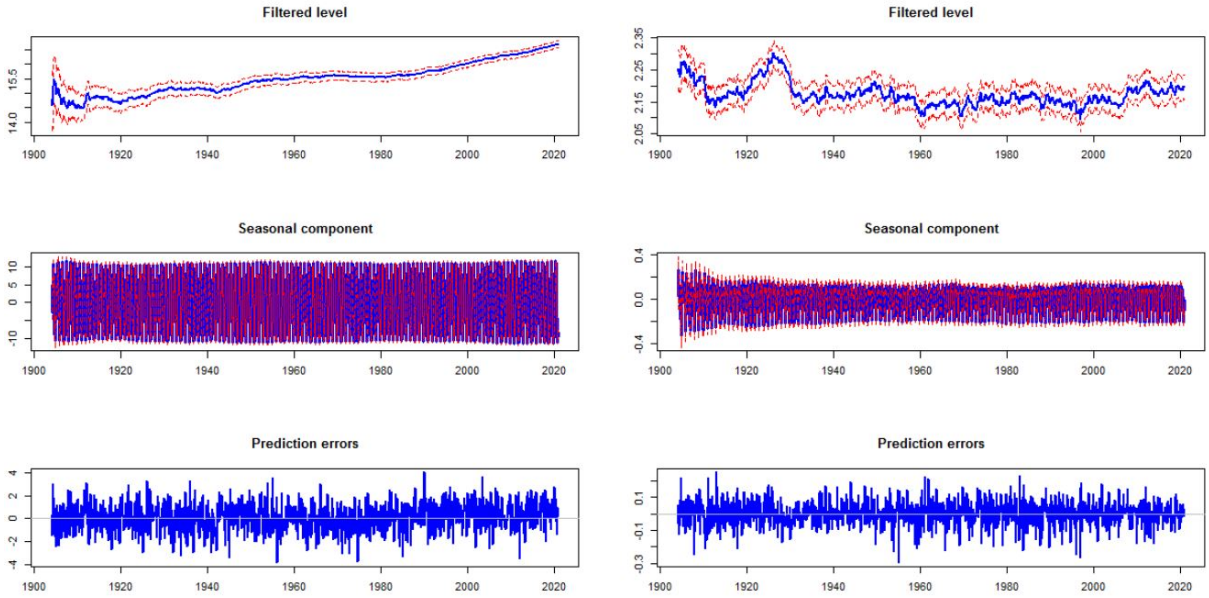

B Joint modelling of center and log-range temperature at selected locations of the Iberian Peninsula

B.1 Barcelona

Table 3: Estimation results of the joint state space model fitted to maximum and minimum temperatures in four locations in the Iberian peninsula.

	Center	Log-range	Cov	Corr	Center	Log-range	Cov	Corr
	Barcelona				Coruña			
Measurement	1.302	0.005	0.015	0.186	1.096	0.017	0.021	0.154
Level	9.29×10^{-23}	2.48×10^{-5}	1.21×10^{-16}	0.003	7.12×10^{-14}	5.67×10^{-5}	-5.65×10^{-13}	-0.000
Slope	1.92×10^{-36}	1.60×10^{-10}	1.73×10^{-23}	0.987	8.33×10^{-8}	1.40×10^{-11}	-6.11×10^{-10}	-0.566
Seasonal 1	1.67×10^{-4}	1.16×10^{-6}	1.62×10^{-7}	0.012	3.99×10^{-7}	3.75×10^{-6}	-1.34×10^{-9}	-0.001
Seasonal 2	1.47×10^{-40}	1.57×10^{-10}	1.52×10^{-25}	1.000	1.50×10^{-44}	4.48×10^{-12}	-2.59×10^{-28}	-0.999
	Madrid				Seville			
Measurement	1.062	0.006	0.011	0.138	0.979	0.006	0.004	0.052
Level	1.47×10^{-19}	1.60×10^{-5}	2.81×10^{-16}	0.004	1.47×10^{-19}	3.39×10^{-5}	1.07×10^{-14}	0.005
Slope	9.99×10^{-8}	2.78×10^{-10}	5.19×10^{-9}	0.98	1.51×10^{-7}	7.89×10^{-10}	1.09×10^{-8}	0.999
Seasonal 1	4.25×10^{-4}	2.07×10^{-6}	3.39×10^{-7}	0.011	3.10×10^{-4}	1.45×10^{-6}	4.91×10^{-7}	0.023
Seasonal 2	3.29×10^{-33}	2.70×10^{-10}	9.42×10^{-22}	0.999	4.45×10^{-36}	7.78×10^{-10}	5.89×10^{-23}	1.002

B.2 Coruña

B.3 Madrid

Table **??** reports the parameter estimates obtained when model (1) is fitted to the center and log-range temperature system in Madrid. The estimates reported in Table **??** imply that $\hat{\sigma}^2_{\eta_1}$ is approximately zero while $\hat{\sigma}^2_{\psi_1}$ is small. Consequently, the center temperature

Figure 11: Diagnostics of standardized residuals of the SSM model for center (top row) and log-range (bottom row) temperature in Barcelona: Q-Q plot (left column) and autocorrelations (right column).

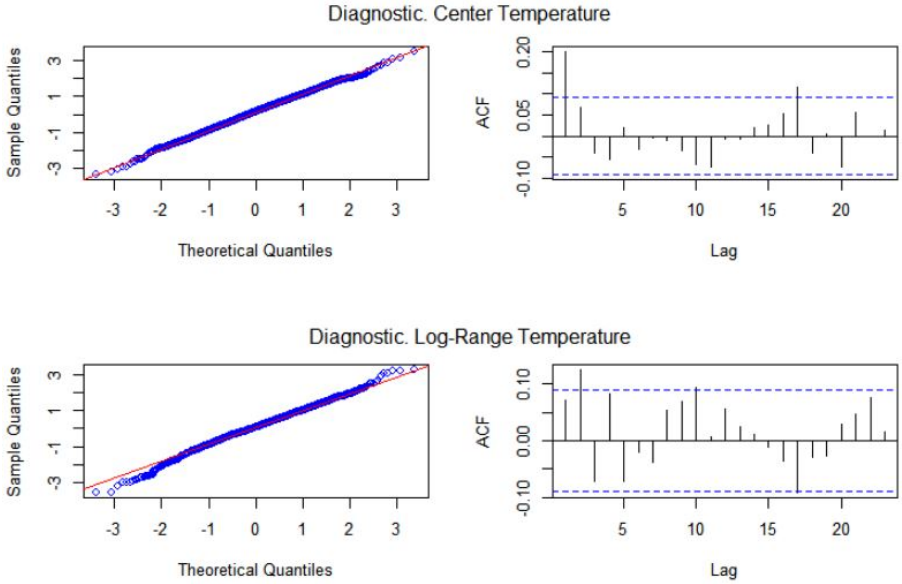

Figure 12: Diagnostics of standardized residuals of the SSM model for center (top row) and log-range (bottom row) temperature in Barcelona: Q-Q plot (left column) and autocorrelations (right column).

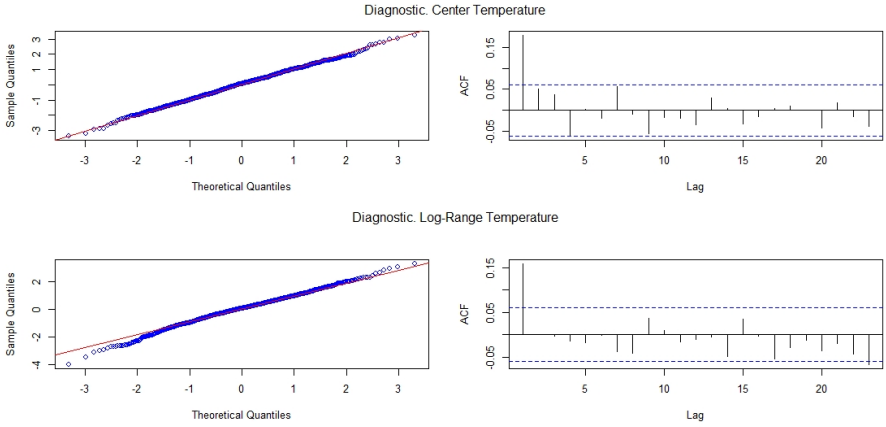

Figure 13: Estimated trend (top row), seasonal (middle row) and irregular (bottom row) of center (left column) and log-range (right column) temperature in Coruña.

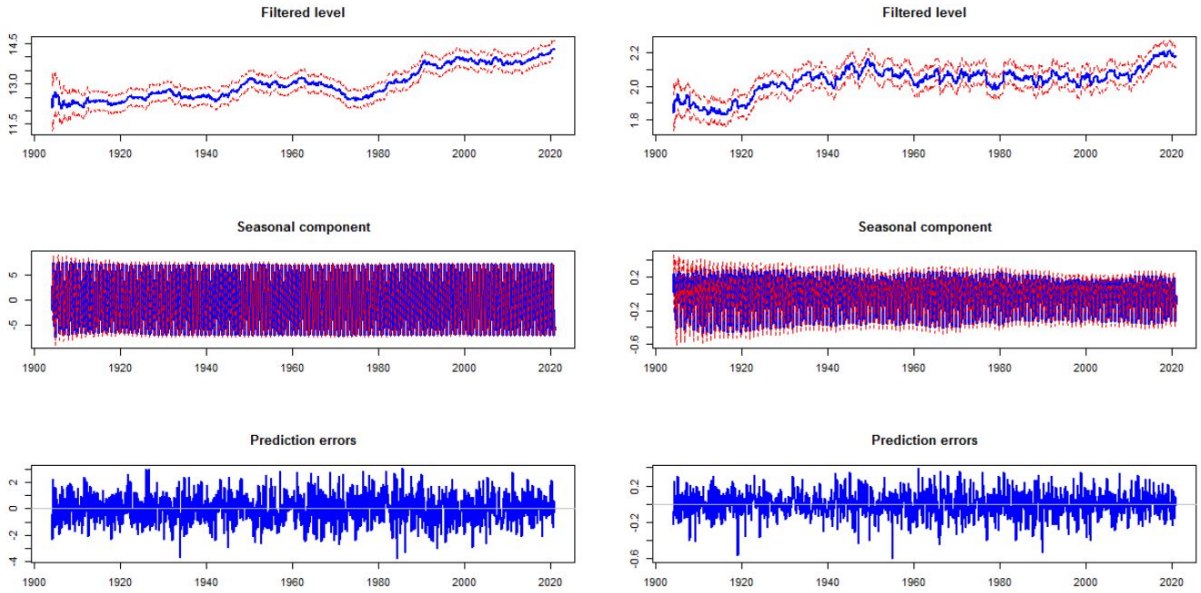

Figure 14: Diagnostics of standardized residuals of the SSM model for center (top row) and log-range (bottom row) temperature in Coruña: Q-Q plot (left column) and autocorrelations (right column).

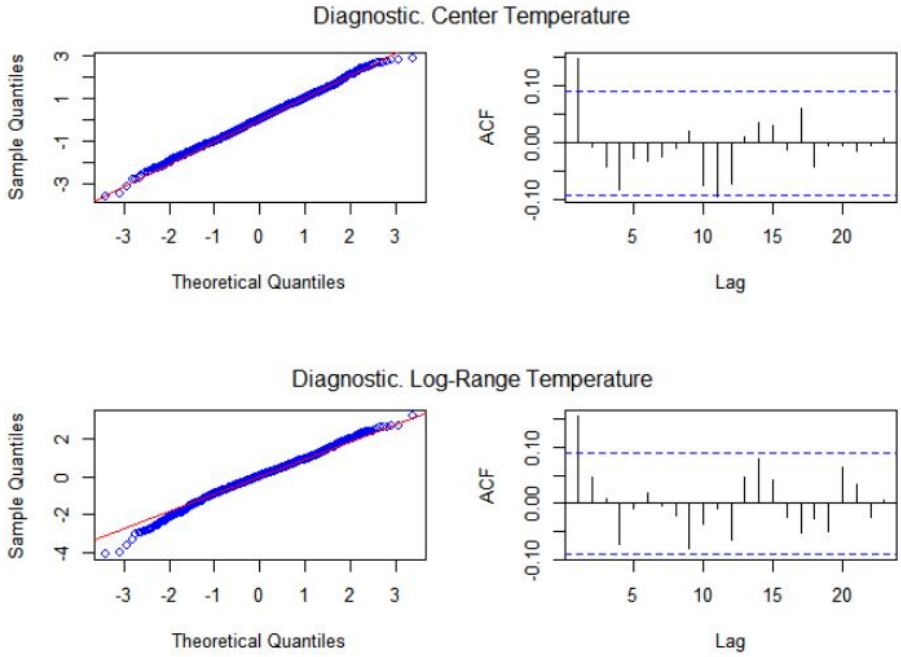

Figure 15: Diagnostics of standardized residuals of the SSM model for center (top row) and log-range (bottom row) temperature in Coruña: Q-Q plot (left column) and autocorrelations (right column).

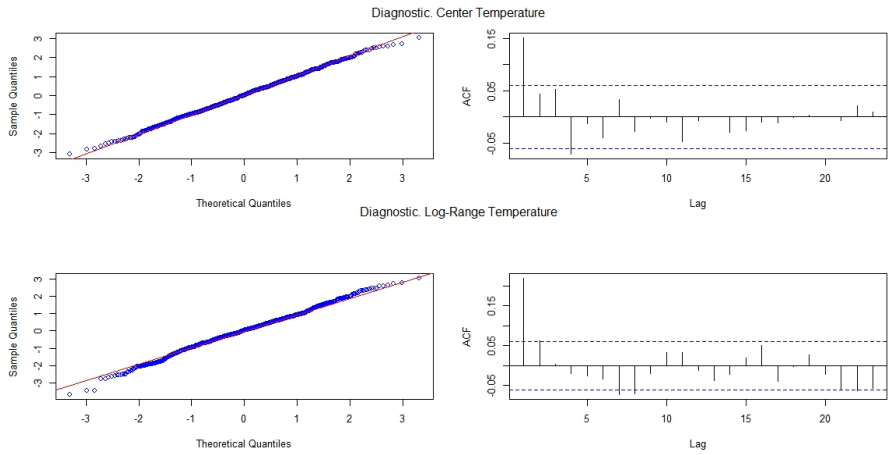

can be well represented by a Integrated Random Walk according to which the trend is smoothly evolving over time. Figure 16, which plots the estimated level, illustrates this smooth evolution of the trend of center temperature. Furthermore, Table **??** shows that $\hat{\sigma}^2_{\omega_1^{(1)}}$ is rather small while $\hat{\sigma}^2_{\omega_1^{(2)}}$ is approximately zero. These estimates are reflected in the very smooth evolution of the seasonal component of center temperature observed in Figure 16. Figure 17, which plots the QQ plots and estimated autocorrelations of the corresponding standardized residuals, does not show any sign of misspecification.

When looking at the results corresponding to the log-range temperature in Madrid, Table **??** shows that all the estimated variances, although small, imply non-negligible signal-to-noise ratios. Therefore, both the trend and seasonal components of log-range temperature in Madrid are stochastic; see also their estimates plotted in Figure 16. The diagnosis of the standardized residuals show that, although mostly uncorrelated, they are characterized by a distribution with heavy tails.

Finally, a final remarkable result observed in Table **??** is that the estimated covariances between the shocks of the center and log-range temperature imply correlations close to zero. Note that although the correlations between the shocks to the slopes of the center and log-range are close to 1, this is due to the extremely small estimated variances. The same happens when looking at the correlation between the shocks to the first seasonal frequency of the center and log-range temperature. An important consequence of this result is that the center and log-range temperature can be modelled separately.

B.4 Seville

B.5 ANALYSIS FROM 1980 TO 2020

Figure 16: Estimated trend (top row), seasonal (middle row) and irregular (bottom row) of center (left column) and log-range (right column) temperature in Madrid.

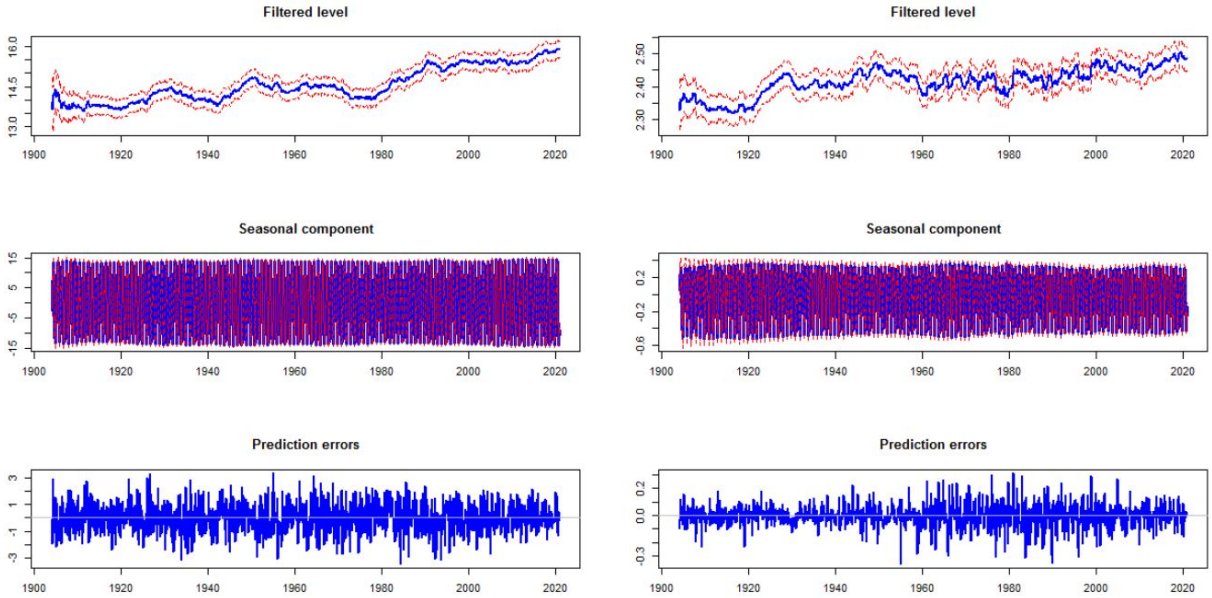

Figure 17: Diagnostics of standardized residuals of the SSM model for center (top row) and log-range (bottom row) temperature in Madrid: Q-Q plot (left column) and autocorrelations (right column).

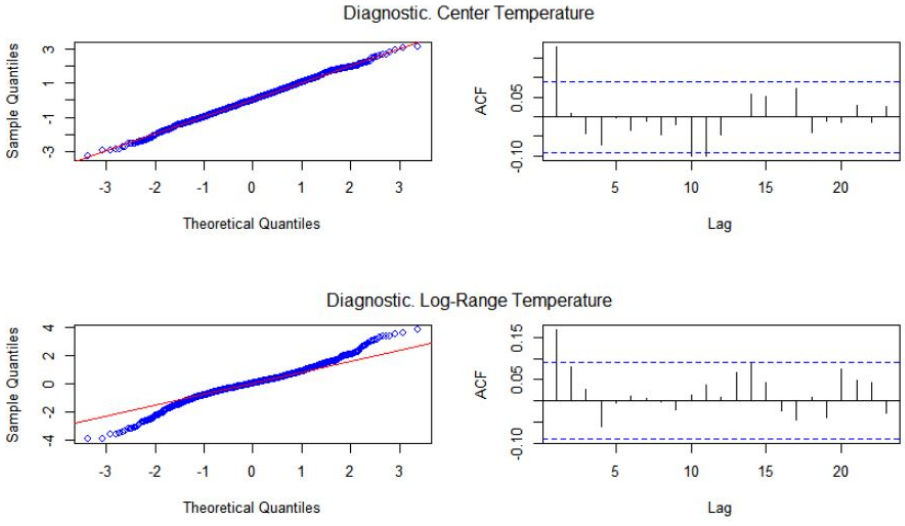

Figure 18: Diagnostics of standardized residuals of the SSM model for center (top row) and log-range (bottom row) temperature in Madrid: Q-Q plot (left column) and autocorrelations (right column).

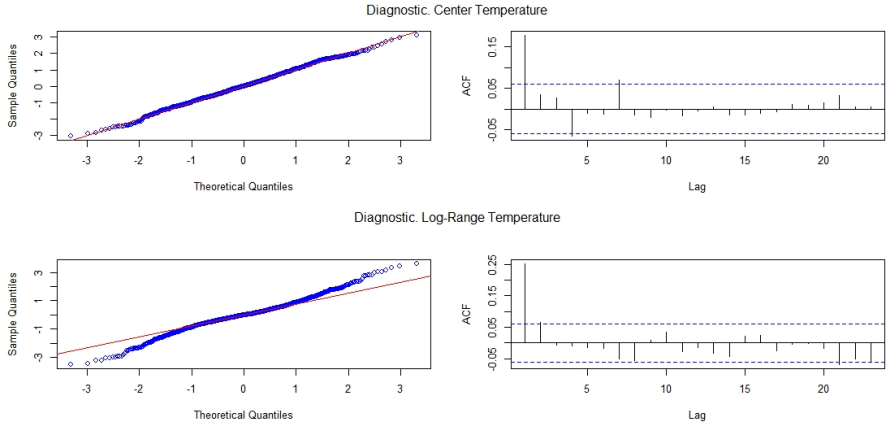

Figure 19: Estimated trend (top row), seasonal (middle row) and irregular (bottom row) of center (left column) and log-range (right column) temperature in Seville.

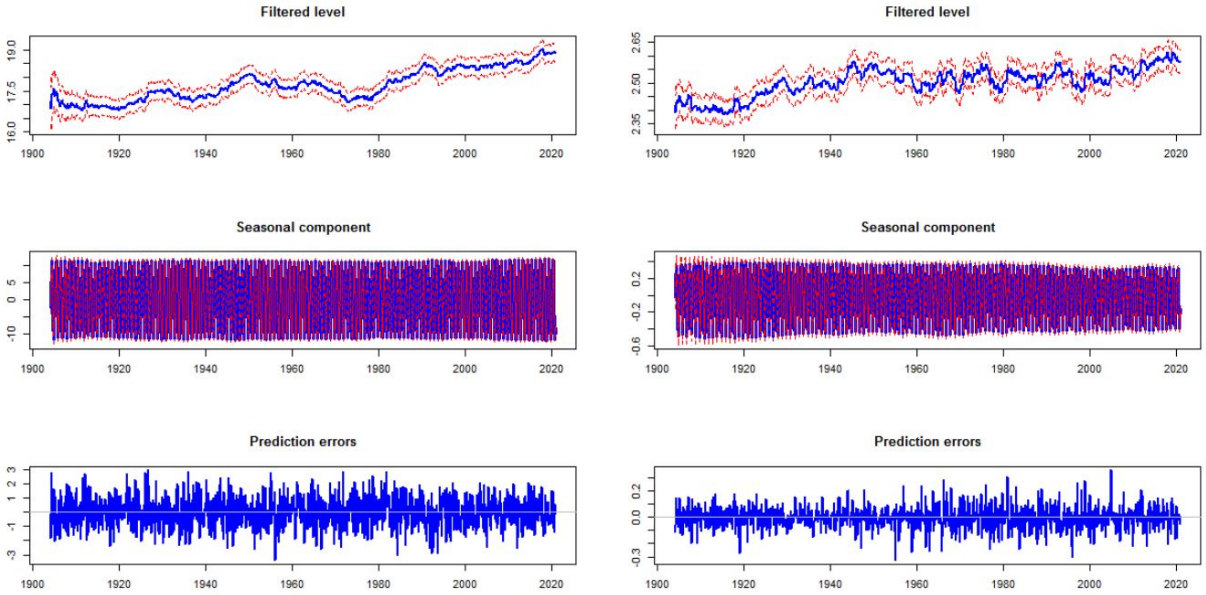

Figure 20: Diagnostics of standardized residuals of the SSM model for center (top row) and log-range (bottom row) temperature in Seville: Q-Q plot (left column) and autocorrelations (right column).

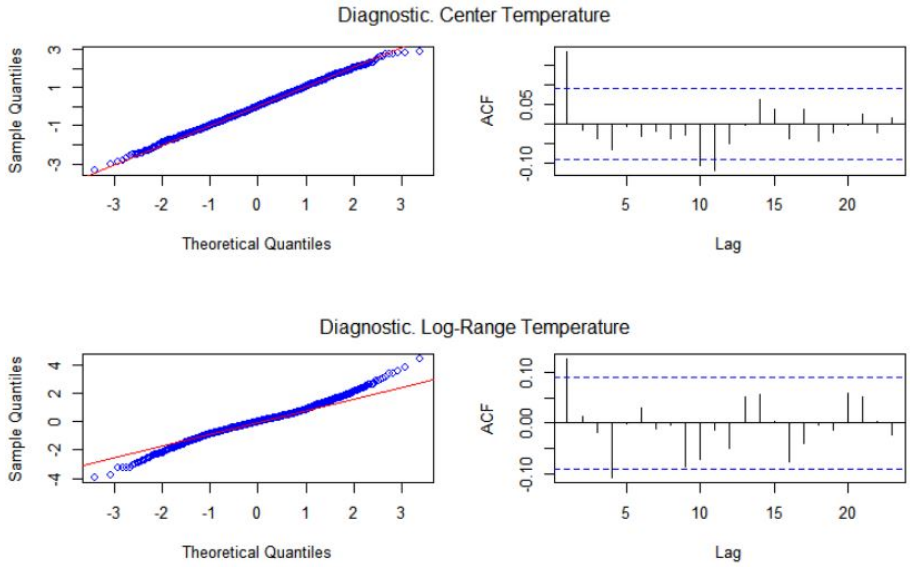

Figure 21: Diagnostics of standardized residuals of the SSM model for center (top row) and log-range (bottom row) temperature in Seville: Q-Q plot (left column) and autocorrelations (right column).

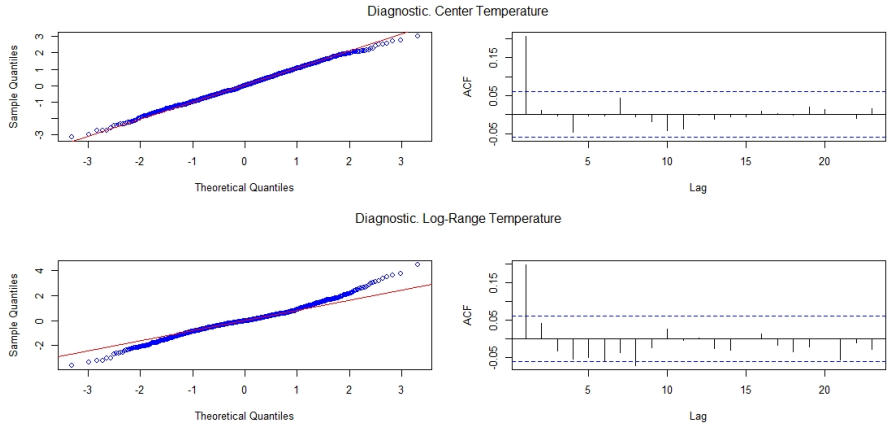

Figure 22: Estimated trend (top row), seasonal (middle row) and irregular (bottom row) of center (left column) and log-range (right column) temperature in Barcelona.

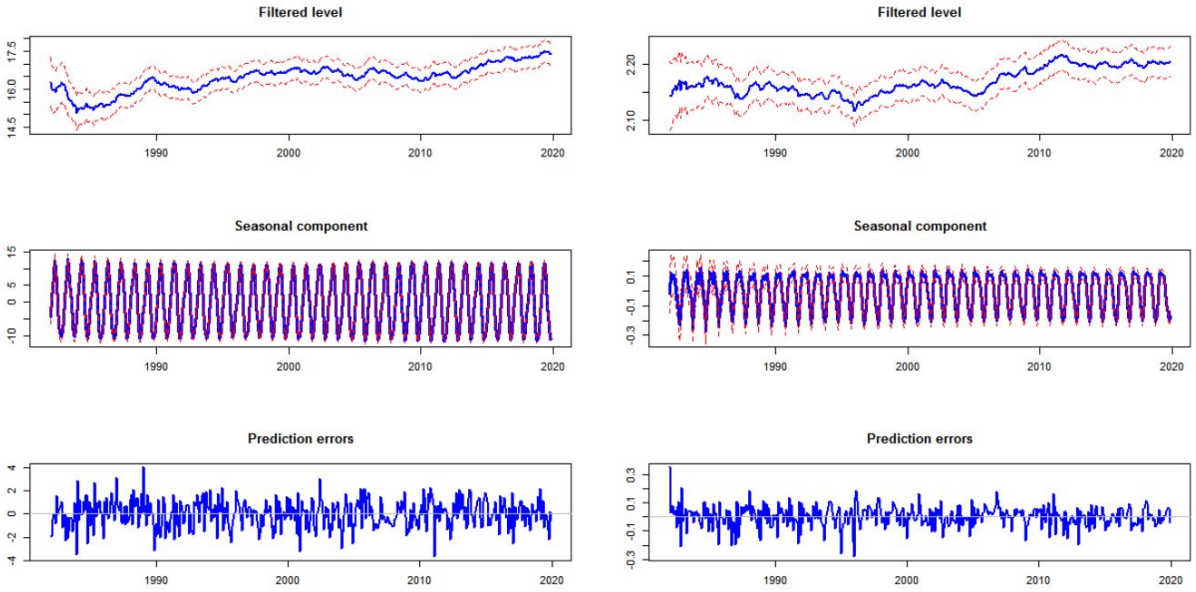

Figure 23: Diagnostics of standardized residuals of the SSM model for center (top row) and log-range (bottom row) temperature in Barcelona: Q-Q plot (left column) and autocorrelations (right column).

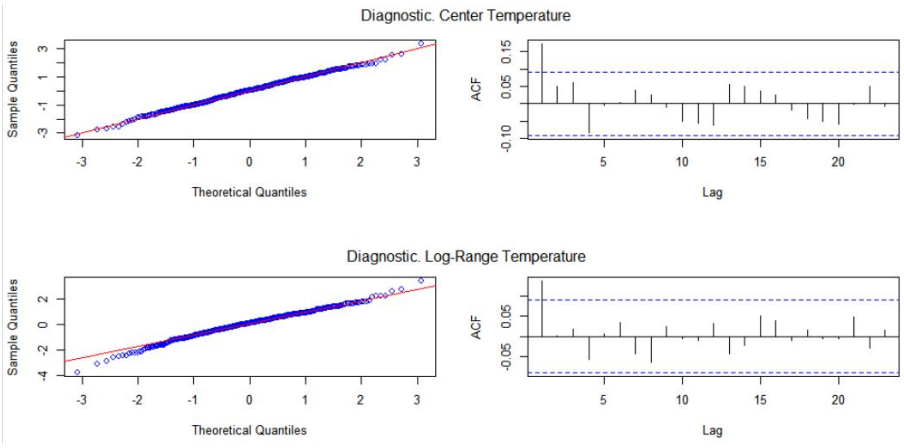

Table 4: Estimation results of the state space model fitted to center and log-range temperatures in four locations in the Iberian peninsula observed from 1980.

	Center	Log-range	Covariance	Correlation	Center	Log-range	Covariance	Correlation
	Barcelona				Coruña			
Measurement	1.252	0.005	0.017	0.215	1.148	0.019	0.027	0.183
Level	3.32×10^{-6}	2.04×10^{-7}	4.94×10^{-8}	0.060	2.16×10^{-4}	4.33×10^{-7}	2.33×10^{-6}	0.241
Slope	6.89×10^{-7}	2.10×10^{-9}	2.25×10^{-8}	0.59	4.33×10^{-10}	2.51×10^{-8}	3.30×10^{-9}	1.001
Seasonal 1	3.62×10^{-4}	3.53×10^{-8}	5.16×10^{-7}	0.144	4.76×10^{-4}	3.46×10^{-6}	2.59×10^{-8}	0.001
Seasonal 2	1.25×10^{-12}	7.36×10^{-10}	3.04×10^{-11}	0.363	1.30×10^{-13}	5.71×10^{-11}	2.51×10^{-8}	-
	Madrid				Seville			
Measurement	1.000	0.008	0.016		0.925	0.006	0.010	
Level	4.61×10^{-7}	8.79×10^{-6}	7.37×10^{-6}		3.38×10^{-6}	4.82×10^{-10}	5.14×10^{-8}	
Slope	7.14×10^{-11}	1.18×10^{-8}	9.17×10^{-10}		8.88×10^{-5}	1.24×10^{-9}	6.14×10^{-10}	
Seasonal 1	8.73×10^{-4}	2.49×10^{-6}	3.21×10^{-6}		1.72×10^{-3}	1.36×10^{-6}	1.16×10^{-6}	
Seasonal 2	7.15×10^{-12}	1.18×10^{-8}	2.90×10^{-10}		1.88×10^{-12}	7.82×10^{-10}	3.84×10^{-11}	